

Bi9393 Analytická cytometrie

Lekce 2



Karel Souček, Ph.D.

Oddělení cytokinetiky
Biofyzikální ústav AVČR, v.v.i
Královopolská 135
612 65 Brno

e-mail: ksoucek@ibp.cz
tel.: 541 517 166


The NK cell receptor NKp46 recognizes ecto-calreticulin on ER-stressed cells

<https://doi.org/10.1038/s41586-023-05912-0>

Received: 13 August 2020

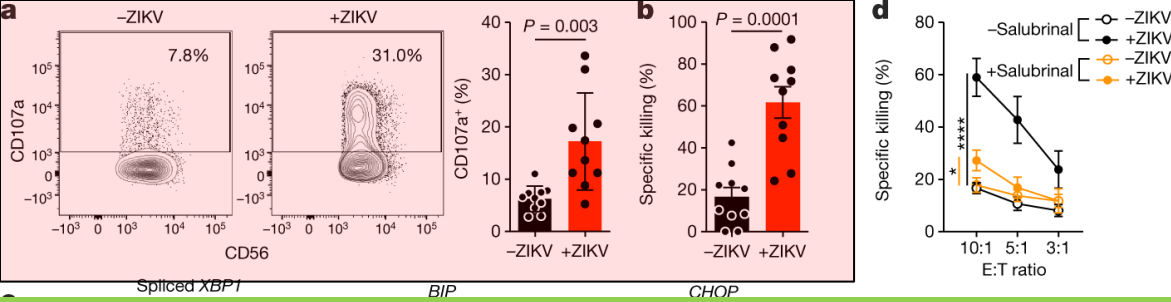
Accepted: 2 March 2023

Published online: 5 April 2023

 Check for updates

Sumit Sen Santara^{1,2,3,9}, Dian-Jang Lee^{1,2,9}, Ângela Crespo^{1,2}, Jun Jacob Hu^{1,4}, Caitlin Walker^{1,4}, Xiyu Ma^{1,2}, Ying Zhang^{1,2}, Sourav Chowdhury⁵, Karla F. Meza-Sosa^{1,2,6}, Mercedes Lewandrowski^{1,2}, Haiwei Zhang^{1,2}, Marjorie Rowe^{1,2}, Arthur McClelland⁷, Hao Wu^{1,4}, Caroline Junqueira^{1,2,8} & Judy Lieberman^{1,2}✉

Natural killer (NK) cells kill infected, transformed and stressed cells when an activating NK cell receptor is triggered¹. Most NK cells and some innate lymphoid cells express the activating receptor NKp46, encoded by *NCRI*, the most evolutionarily ancient NK cell receptor^{2,3}. Blockage of NKp46 inhibits NK killing of many cancer targets⁴. Although a few infectious NKp46 ligands have been identified, the endogenous NKp46 cell surface ligand is unknown. Here we show that NKp46 recognizes externalized calreticulin (ecto-CRT), which translocates from the endoplasmic reticulum (ER) to the cell membrane during ER stress. ER stress and ecto-CRT are hallmarks of chemotherapy-induced immunogenic cell death^{5,6}, flavivirus infection and senescence. NKp46 recognition of the P domain of ecto-CRT triggers NK cell signalling and NKp46 caps with ecto-CRT in NK immune synapses. NKp46-mediated killing is inhibited by knockout or knockdown of *CALR*, the gene encoding CRT, or CRT antibodies, and is enhanced by ectopic expression of glycosylphosphatidylinositol-anchored CRT. *NCRI*-deficient human (and *Ncr1*-deficient mouse) NK cells are impaired in the killing of ZIKV-infected, ER-stressed and senescent cells and ecto-CRT-expressing cancer cells. Importantly, NKp46 recognition of ecto-CRT controls mouse B16 melanoma and RAS-driven lung cancers and enhances tumour-infiltrating NK cell degranulation and cytokine secretion. Thus, NKp46 recognition of ecto-CRT as a danger-associated molecular pattern eliminates ER-stressed cells.



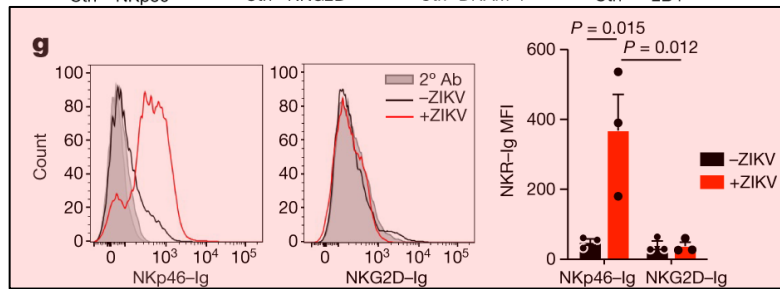
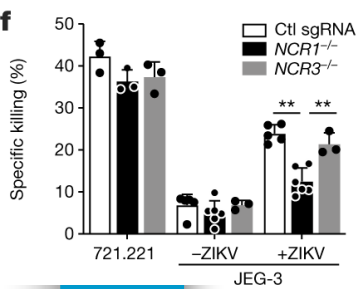
a, Representative flow cytometry plots (left) and percentage of degranulating NK cells isolated from the blood of ten healthy donors (right), as measured by surface CD107a, in response to uninfected and ZIKV-infected JEG-3 cells (8 h coculture, E:T ratio 1:3). **b**, NK cell-specific killing of uninfected and ZIKV-infected JEG-3 cells.

c, ER stress, as assessed by *XBP1* splicing (left) and increases in *BIP* (middle) and *CHOP* (right) mRNA, in JEG-3 cells that were uninfected or infected with ZIKV, HSV-2 or human cytomegalovirus (HCMV) for 1–2 days or treated with tunicamycin (Tu) for 1 day. Indicated samples were pretreated with the ER stress inhibitor salubrinal ($n = 3$ samples). mRNA levels, as assayed by quantitative PCR with reverse transcription (RT-qPCR), were normalized to *ACTB*. **d**, Effect of salubrinal pretreatment of target cells on NK cell killing of ZIKV-infected (top) and tunicamycin-treated (bottom) JEG-3 cells ($n = 6$ samples). **e**, Effect of NKR-blocking antibodies (Ab) on NK cell killing of uninfected or ZIKV-infected JEG-3 cells ($n = 3–7$ samples). Ctrl, control. **f**, Specific killing of the classical NK cell target 722.221 cells, or of uninfected or ZIKV-infected JEG-3 cells by human NK cell line YT cells knocked out for *NCR1* or *NCR3* or treated with control single-guide RNAs ($n = 3–6$ samples).

g, Representative flow cytometry histogram (left) and mean fluorescence intensity (MFI) of NKR-Ig fusion protein (Nkp46-Ig and NKG2D-Ig) binding to uninfected or ZIKV-infected JEG-3 cells (right) ($n = 3$ samples). **b,d–f**, Specific killing assessed by 8 h ^{51}Cr release assay using an E:T ratio of 10:1 unless otherwise indicated. Data are mean \pm s.e.m. of at least three independent experiments or technical replicates. Statistics were performed using two-tailed, nonparametric, unpaired *t*-test (**a,b**), one-way analysis of variance (ANOVA) (**c**), two-way ANOVA (**e–g**) or area under the curve followed by one-way ANOVA (**d**). * $P < 0.05$, ** $P < 0.01$, *** $P < 0.001$, **** $P < 0.0001$.

-CD56 is a single transmembrane glycoprotein also known as N-CAM (Neural Cell Adhesion Molecule), Leu-19, or NKH1. It is a member of the Ig superfamily. The 140 kD isoform is expressed on NK cells and NK-T cells. CD56 is also expressed in the brain (cerebellum and cortex) and at neuromuscular junctions.

-lysosomal-associated membrane protein-1 (LAMP-1 or CD107a) has been described as a marker of CD8+ T-cell degranulation following stimulation.



nature

Explore content About the Journal Publish with us

nature > articles > article

Article | Published: 05 April 2023

The NK cell receptor Nkp46 recognizes ectocalreticulin on ER-stressed cells

Sumit Sen-Santora, Dian-Jang Lee, Angela Crespo, Jun-Jacob Hu, Caitlin Walker, Xiu-Ma Ying, Zhao-Sourav Chowdhury, Karla F. Meza-Sosa, Mercedes Lewandrowski, Haiwei Zhang, Marjorie Rowe, Arthur McClelland, Hao-Yu Caroline Junqueira & Judy Lieberman

Nature 616, 348–356 (2023) | Cite this article

17k Accesses | Citations | 99 Altmetric | Metrics

The NK cell receptor NKP46 recognizes ectocalreticulin on ER-stressed cells

Sumit Sen Santara, Dian-Jiang Lee, Angela Crespo, Jun-Jacob Hu, Caitlin Walker, Xinyi Ma, Ying Zhang,

Sourav Choudhury, Karla F. Mesa-Sosa, Mercedes Lewandrowski, Haiwei Zhang, Marjorie Rowe, Arthur

McClelland, Hao Wu, Caroline Junqueira  & Judy Lieberman 

Nature 616, 348–356 (2023) | [Cite this article](#)

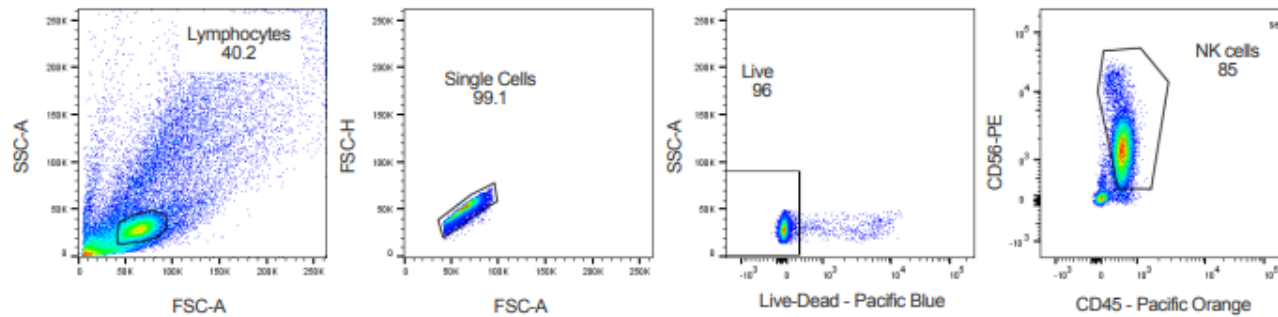
17k Accesses | 8 Citations | 99 Altmetric | [Metrics](#)

Flow cytometry

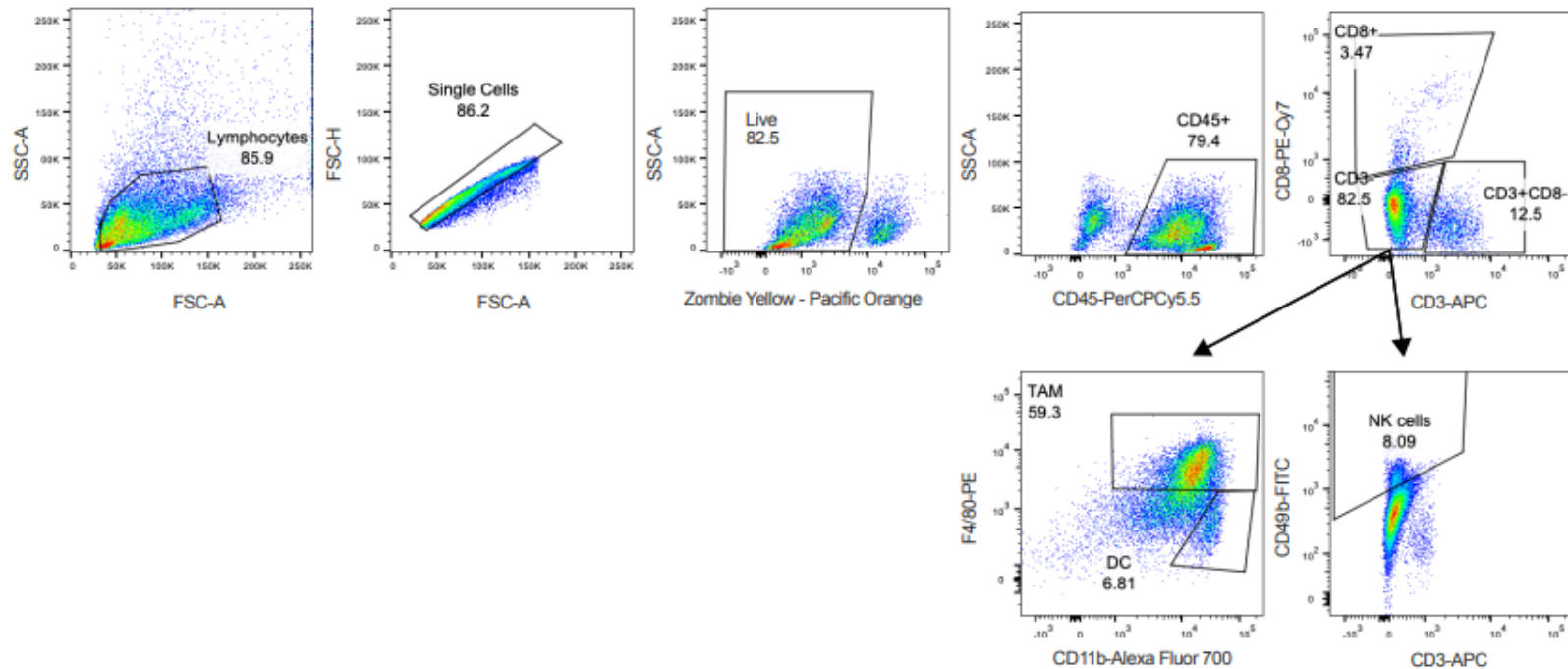
For surface staining, cells were stained for 30 min on ice in the dark with LIVE/DEAD-Violet stain (1:1,000) and then with primary antibodies for 15–30 min in PBS and 2% FCS (followed by secondary antibodies, when applicable, for 20 min). For protein–Ig staining, cells were incubated with 50 $\mu\text{g ml}^{-1}$ fusion protein for 1 h at 4 °C and then stained with fluorescent-anti-human IgG for 1 h. Cells were fixed in 1% paraformaldehyde (Affymetrix) for 10 min before flow cytometry. Flow cytometry was assessed on gated live cells (Supplementary Fig. [1](#)). For intracellular staining, cells were fixed and permeabilized using the CytoFix/CytoPerm kit. One of the treated samples was used for isotype staining, and MFI of staining with the isotype control antibody was subtracted from MFI of the specific antibody. Analysis was performed on a FACSCanto II (BD). BD FACSDiva 8.0 (BD) software was used for data collection, with analysis performed using FlowJo v.10.4.2 (TreeStar).

Supplementary Figure 1 | Flow cytometry gating strategy

a. Peripheral blood NK or YT NK cultured with JEG-3.



b. Tumor infiltrating lymphocytes (TILs) from tumor-bearing mice



Comment



ILLUSTRATIONS BY DAVID PARKINS

Replication games: how to make reproducibility research more systematic

Abel Brodeur, Anna Dreber, Fernando Hoces de la Guardia & Edward Miguel

In some areas of social science, around half of studies can't be replicated. A new test-fast, fail-fast initiative aims to show what research is hot – and what's not.

In October last year, one of us (A.B.) decided to run an ad hoc workshop at a research centre in Oslo, to try to replicate papers from economics journals. Instead of the handful of locals who were expected to attend, 70 people from across Europe signed up. The message was clear: researchers want to replicate studies.

Replication is sorely needed. In areas of the social sciences, such as economics, philosophy and psychology, some studies suggest that between 35% and 70% of published results cannot be replicated when tested with

new data¹⁻⁴. Often, researchers cannot even reproduce results when using the same data and code as the original paper, because key information is missing.

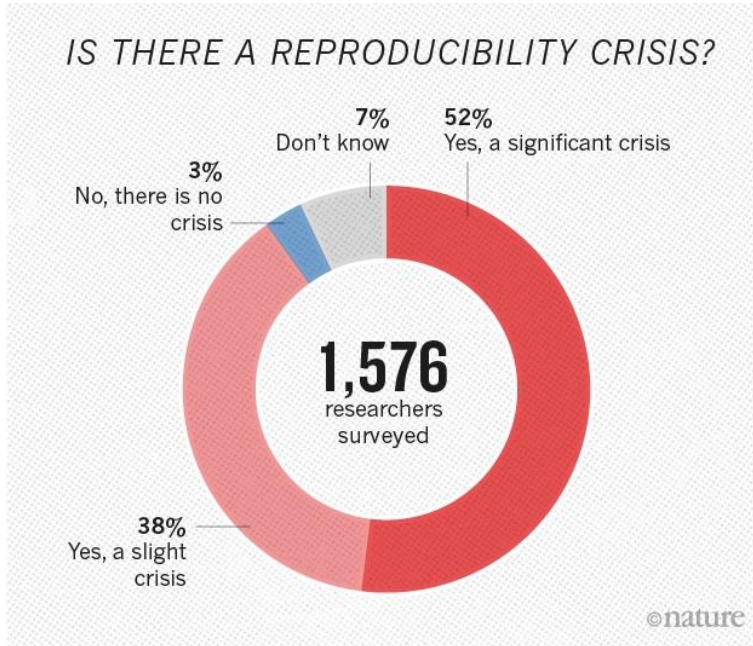
Yet most journals will not publish a replication unless it refutes an impactful paper. In economics, less than 1% of papers published in the top 50 journals between 2010 and 2020 were some type of replication⁵. That suggests that many studies with errors are going undetected.

After the Oslo workshop, we decided to try to make replication efforts in our fields of economics and political science more systematic.

Reprodukovatelnost výsledků

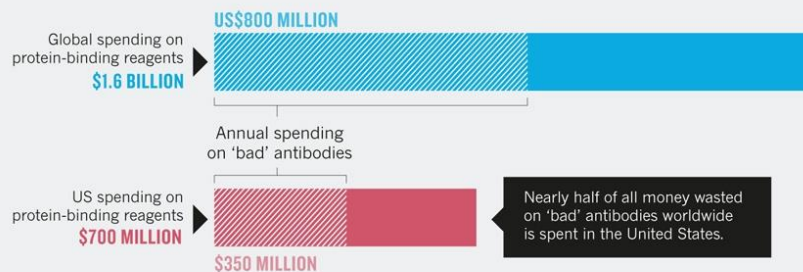
Nature 533, 452–454 (26 May 2016)

doi:10.1038/533452a



MONEY DOWN THE DRAIN

The use of poorly characterized and ill-defined antibodies wastes materials, researcher time and money.

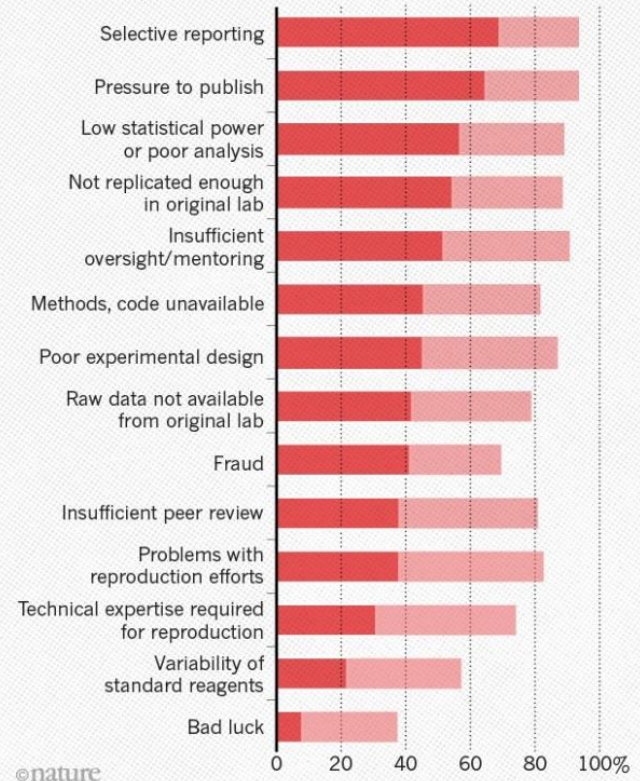


All costs estimates assume that 50% of antibodies are validated and that researchers buy 'bad' antibodies as often as they buy 'good' ones.

WHAT FACTORS CONTRIBUTE TO IRREPRODUCIBLE RESEARCH?

Many top-rated factors relate to intense competition and time pressure.

● Always/often contribute ● Sometimes contribute



[Circ Res.](#) 2015 Jan 2;116(1):116-26. doi: 10.1161/CIRCRESAHA.114.303819.

Reproducibility in science: improving the standard for basic and preclinical research.

[Begley CG](#)¹, [Ioannidis JP](#)².

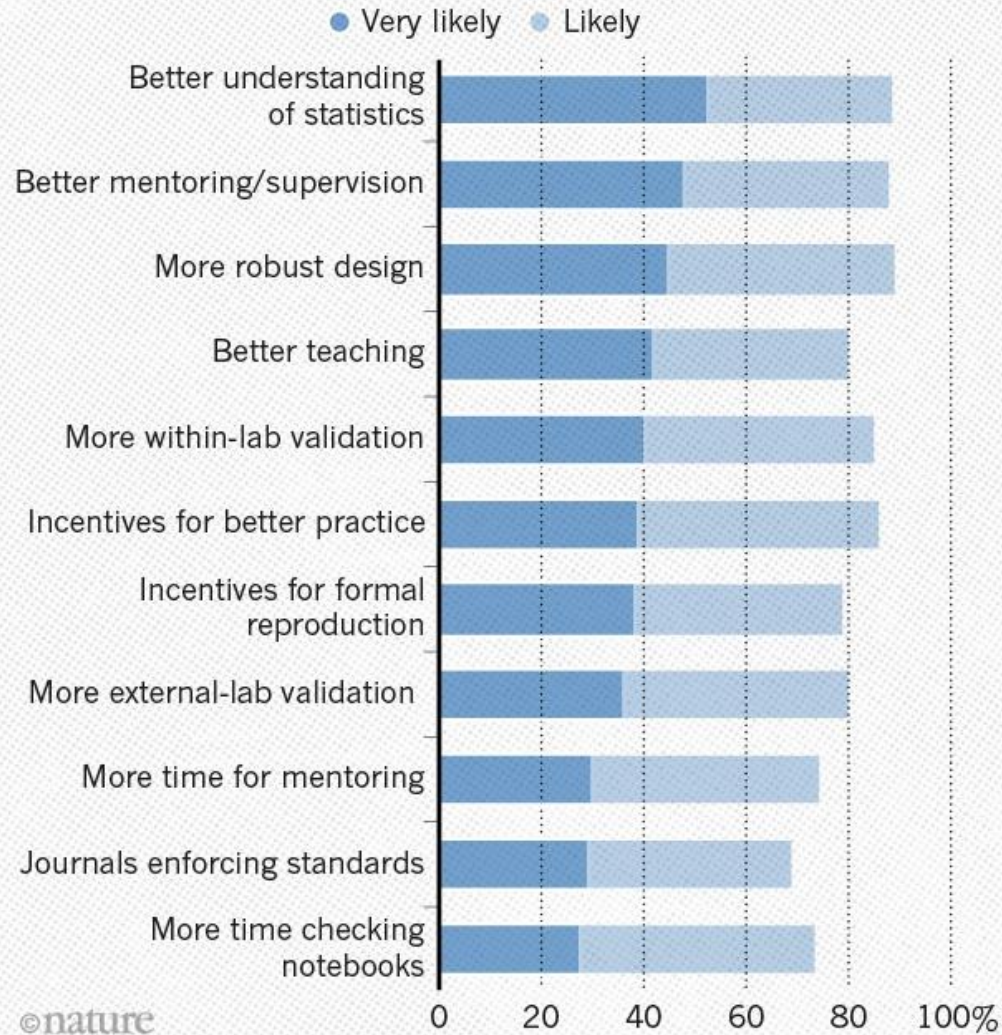
[Nature.](#) 2015 Feb 5;518(7537):27-9. doi: 10.1038/518027a.

Reproducibility: Standardize antibodies used in research.

[Bradbury A](#)¹, [Plückthun A](#)².

WHAT FACTORS COULD BOOST REPRODUCIBILITY?

Respondents were positive about most proposed improvements but emphasized training in particular.



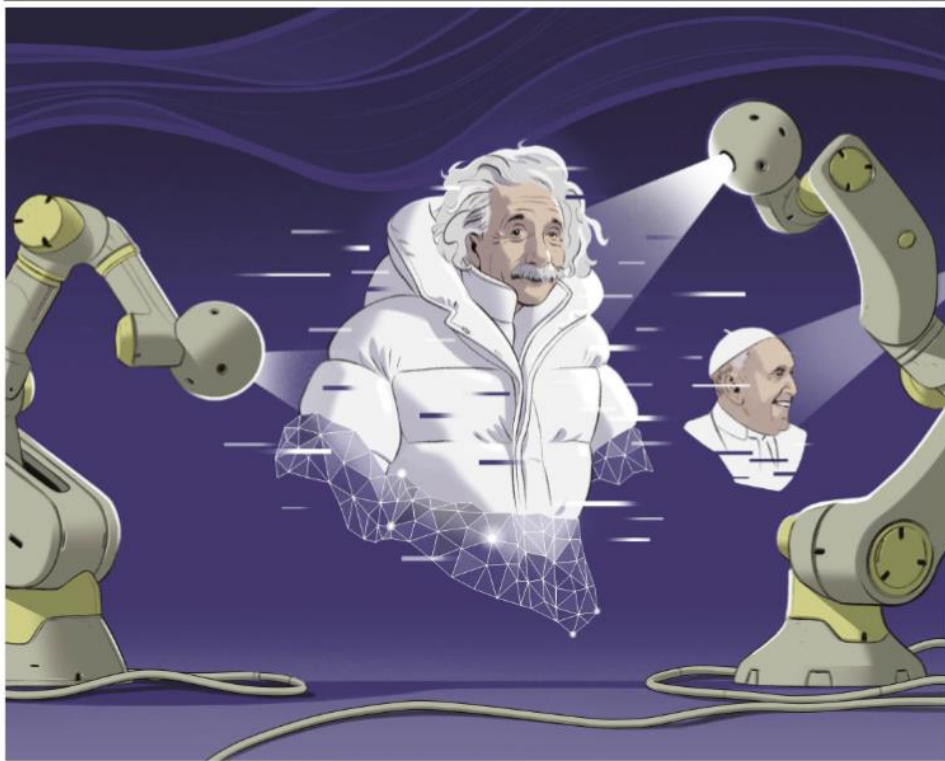


ILLUSTRATION BY STEVE HAHNE

HOW TO STOP DEEPFAKES FROM SINKING THE INTERNET

Deceptive videos and images created using generative AI could sway elections, crash stock markets and ruin reputations. Researchers are developing methods to limit their harm. **By Nicola Jones**

This June, in the political battle leading up to the 2024 US presidential primaries, a series of images were released showing Donald Trump embracing one of his former medical advisers, Anthony Fauci. In a few of the shots, Trump is captured awkwardly kissing the face of Fauci,

a health official reviled by some US conservatives for promoting masking and vaccines during the COVID-19 pandemic.

"It was obvious" that they were fakes, says Hany Farid, a computer scientist at the University of California, Berkeley, and one of many specialists who examined the pictures. On close inspection of three of the photos,

Trump's hair is strangely blurred, the text in the background is nonsensical, the arms and hands are unnaturally placed and the details of Trump's visible ear are not right. All are hallmarks – for now – of generative artificial intelligence (AI), also called synthetic AI.

Such deepfake images and videos, made by text-to-image generators powered by 'deep



PEOPLE'S ABILITY TO REALLY KNOW WHERE THEY SHOULD PLACE THEIR TRUST IS FALLING AWAY."

R
S
F
C
H
I

R
D
L
C
N
C
A
A

Scammed science

What can researchers do to limit the impact of fake images on science?

Science isn't immune to the problem of AI-generated fakery. One concern is the integrity of biomedical images such as scans, microscopy images and western blots – a standard technique in which distinctive bands are created by proteins of various molecular weights as they spread across a gel. Fraudsters have long faked such images using Photoshop or other image-manipulation software, but that is often detectable by a trained eye or by computers that check for image duplication. Generating images entirely with AI presents a bigger detection problem.

Last year, Rongshan Yu and his colleagues at Xiamen University, China, created scientific images using synthetic AI to see how easily it can be done. They trained one generative AI program to create new western blot images from a training data set of 3,000 images; and used another to insert features of oesophageal cancer into an image of a non-cancerous intestine. They then tested how convincing the western blots were by inviting three specialists to try to spot one fake in a set of four images; two of the experts performed worse than chance, and the third fared better by spotting a visual clue to do with the smoothness between the image and the background. A computer system did slightly better than the specialists.

In a larger study of 14,000 original western blot images and 24,000 synthetic ones, made using four different generators, Anderson Rocha at the University of Campinas, Brazil, and his colleagues found that AI detectors trained on large data sets achieved accuracies of more than 85% (ref. 8). "This is just the beginning, where we showed it's feasible. It's possible to do way

more than that," Rocha says. He and his team have a paper under review that extends their methods beyond western blots, he says.

No one *Nature* spoke to could provide proof that AI is being used by academics to beef up their papers or funding applications, but experts say it's likely. Wael Abd-Elmaged, an information scientist and computer engineer at the University of Southern California in Los Angeles, says he knows of specific cases in which academics have used AI to synthesize fakes, but declined to divulge details. Researchers investigating fake paper mills have said they have seen

"I don't know any case yet of a retracted paper that used synthetic creation to illustrate the results in that paper," says Rocha, who is working with the blog Retraction Watch on this issue. "But it's just a matter of time, I guess."

Watermarking previously prevent AI and prevent says he pla makers and discuss the provenance Beyond o tools again encourage science. At could be t

"I don't know any case yet of a retracted paper that used synthetic creation to illustrate the results in that paper," says Rocha, who is working with the blog Retraction Watch on this issue. "But it's just a matter of time, I guess."

A proposal for validation of antibodies

Mathias Uhlen¹, Anita Bandrowski², Steven Carr³, Aled Edwards⁴, Jan Ellenberg⁵, Emma Lundberg¹, David L Rimm⁶, Henry Rodriguez⁷, Tara Hiltke⁷, Michael Snyder⁸ & Tadashi Yamamoto⁹

We convened an *ad hoc* International Working Group for Antibody Validation in order to formulate the best approaches for validating antibodies used in common research applications and to provide guidelines that ensure antibody reproducibility. We recommend five conceptual ‘pillars’ for antibody validation to be used in an application-specific manner.

Table 1 | Proposed conceptual pillars for validation of antibodies

| Validation strategy | Genetic | Orthogonal | Independent antibody | Tagged protein expression | IMS |
|---------------------------------|---|---|---|--|--|
| Validation principle | The expression of the target protein is eliminated or significantly reduced by genome editing or RNA interference | Expression of the target protein is compared with an antibody-independent method | Expression of the target protein is compared using two antibodies with nonoverlapping epitopes | The target protein is expressed using a tag, preferably expressed at endogenous levels | The target protein is captured using an antibody and analyzed using MS |
| Validation criteria | Elimination or significant reduction in antibody labeling after gene disruption or mRNA knockdown | Significant correlation of protein levels detected by an antibody and an orthogonal method (e.g., MS) | Significant correlation of protein levels detected by two different antibodies recognizing independent regions of the same target protein | Significant correlation between antibody labeling and detection of the epitope tag | Target protein peptides among the most abundant detected by MS following immunocapture |
| Suitable for these applications | WB, IHC, ICC, FS, SA, IP/ChIP, RP | WB, IHC, ICC, FS, SA, RP | WB, IHC, ICC, FS, SA, IP/ChIP, RP | WB, IHC, ICC, FS | IP/ChIP |

WB, western blot; IHC, immunohistochemistry; ICC, immunocytochemistry, including immunofluorescence microscopy; FS, flow sorting and analysis of cells; SA, sandwich assays, including ELISA; IP, immunoprecipitation; ChIP, chromatin immunoprecipitation; and RP, reverse-phase protein arrays.

CST Antibody Validation Principles



Hallmark Strategy

Description



Binary Model: Antibody signal is measured in model systems with known presence/absence of target signal. Includes wild-type vs. genetic knockout, targeted induction or silencing.



Ranged Expression: Antibody signal strength is measured in cell lines or tissues representing a known continuum of target expression levels. Includes siRNA and heterozygous knockout assays.



Orthogonal Data: Antibody signal is correlated to target expression in model systems measured using antibody independent assays. Includes mass spectrometry and in situ hybridization.



Multiple Antibodies: Antibody signal is compared to the signal observed using antibodies targeting nonoverlapping epitopes of the target. Includes IP, ChIP, and ChIP-seq.



Heterologous Expression: Antibody signal is evaluated in cell lines following heterologous expression of native (or mutated) target protein.



Complementary Assays: Antibody specificity may be validated using complementary assays. Includes competitive ELISA, peptide dot blots, peptide blocking, or protein arrays.

Refine Results

Search Within

CLEAR ALL

Category

- Research
- Cancer (1)
 - Cell Biology (1)
 - Fibrosis (4)
 - Immunology and Immuno-Oncology (4)
 - Metabolism (1)
 - Neuroscience (4)
 - All Research Areas

- Application
- Flow Cytometry (Fixed/Permeabilized) (1)
 - Flow Cytometry (Live) (1)
 - IHC-paraffin (1)
 - Immunofluorescence (Immunocytochemistry) (1)
 - Western blot (3)

Products (4)
Content (1)

Sort By: Relevance

| # | Product Name | Application | Reactivity | |
|-------|--------------------------------------|---|------------|---|
| 98327 | CD9 (E8L5J) Rabbit mAb | WB IP IHC IF F ChIP | M, R | <input type="checkbox"/> COMPARE ADD |
| 13403 | CD9 (D3H4P) Rabbit mAb | WB IP IHC IF F ChIP | H | <input type="checkbox"/> COMPARE ADD |
| 13174 | CD9 (D8O1A) Rabbit mAb | WB IP IHC IF F ChIP | H | <input type="checkbox"/> COMPARE ADD |
| 74220 | Exosomal Marker Antibody Sampler Kit | | | <input type="checkbox"/> COMPARE ADD |

Results per page: 30 60 100 200

CD9 (E8L5J) Rabbit mAb

Cell Signaling
TECHNOLOGY®Orders: 877-616-CELL (2355)
orders@cellsignal.com

Support: 877-678-TECH (8324)

Web: info@cellsignal.com
www.cellsignal.com

3 Trask Lane | Danvers | Massachusetts | 01923 | USA

For Research Use Only. Not For Use In Diagnostic Procedures.

| Applications: | Reactivity: | Sensitivity: | MW (kDa): | Source/Isotype: | UniProt ID: | Entrez-Gene Id: |
|------------------------|-------------|--------------|-----------|-----------------|-------------|-----------------|
| WB, IF-IC, FC-FP, FC-L | M R | Endogenous | 22-27 | Rabbit IgG | P40240 | 12527 |

Product Usage Information

| Application | Dilution |
|--|--------------|
| Western Blotting | 1:1000 |
| Immunofluorescence (Immunocytochemistry) | 1:50 |
| Flow Cytometry (Fixed/Permeabilized) | 1:50 - 1:200 |
| Flow Cytometry (Live) | 1:50 - 1:200 |

Storage

Supplied in 10 mM sodium HEPES (pH 7.5), 150 mM NaCl, 100 µg/ml BSA, 50% glycerol and less than 0.02% sodium azide. Store at -20°C. Do not aliquot the antibody.

Specificity / Sensitivity

CD9 (E8L5J) Rabbit mAb recognizes endogenous levels of total CD9 protein.

Species Reactivity:
Mouse, Rat

Source / Purification

Monoclonal antibody is produced by immunizing animals with a synthetic peptide corresponding to residues surrounding Leu119 within the extracellular domain of mouse CD9 protein.

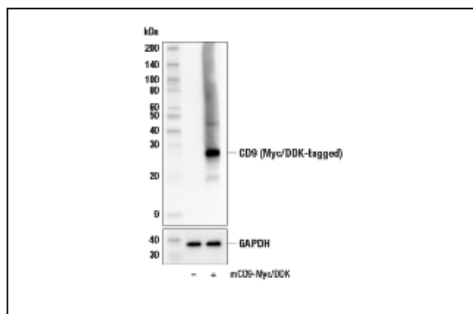
Background

The CD9 antigen belongs to the tetraspanin family of cell surface glycoproteins, and is characterized by four transmembrane domains, one short extracellular domain (ECL1), and one long extracellular domain (ECL2). Tetraspanins interact with a variety of cell surface proteins and intracellular signaling molecules in specialized tetraspanin-enriched microdomains (TEMs), where they mediate a range of processes including adhesion, motility, membrane organization, and signal transduction (1). Research studies demonstrate that CD9 expression on the egg is required for gamete fusion during fertilization (2-4). CD9 was also shown to play a role in dendritic cell migration, megakaryocyte differentiation, and homing of cord blood CD34+ hematopoietic progenitors to the bone marrow (5-7). In addition, downregulation of CD9 expression is associated with poor prognosis and progression of several types of cancer (8-10). Additional research identified CD9 as an abundant component of exosomes, and may play some role in the fusion of these secreted membrane vesicles with recipient cells (11).

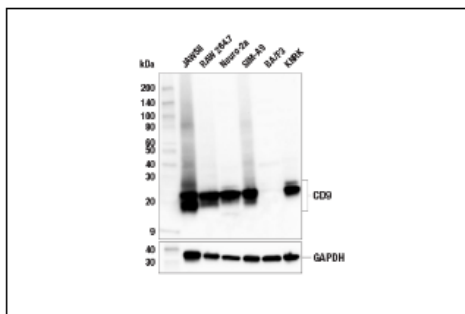
- Hemler, M.E. (2005) *Nat Rev Mol Cell Biol* 6, 801-11.
- Le Naour, F. et al. (2000) *Science* 287, 319-21.
- Miyado, K. et al. (2000) *Science* 287, 321-4.
- Kaji, K. et al. (2000) *Nat Genet* 24, 279-82.
- Mantegazza, A.R. et al. (2004) *Blood* 104, 1183-90.
- Clay, D. et al. (2001) *Blood* 97, 1982-9.
- Leung, K.T. et al. (2011) *Blood* 117, 1840-50.
- Miyake, M. et al. (1995) *Cancer Res* 55, 4127-31.
- Higashiyama, M. et al. (1995) *Cancer Res* 55, 6040-4.
- Uchida, S. et al. (1999) *Br J Cancer* 79, 1168-73.
- Théry, C. et al. (1999) *J Cell Biol* 147, 599-610.

#98327

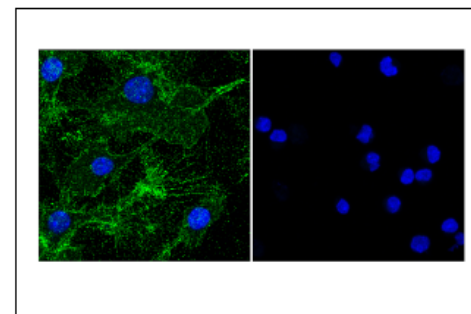
CD9 (E8L5J) Rabbit mAb



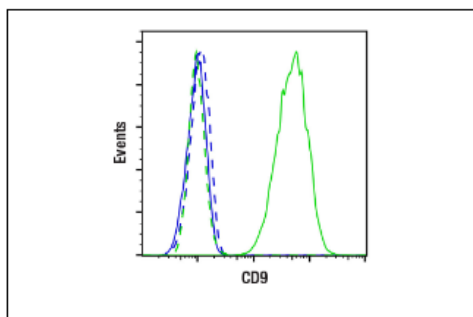
Western blot analysis of extracts from 293T cells, mock transfected (-) or transfected with a construct expressing Myc/DDK-tagged full-length mouse CD9 protein (mCD9-Myc/DDK; +), using CD9 (E8L5J) Rabbit mAb (upper) and GAPDH (D16H11) XP® Rabbit mAb #5174 (lower).



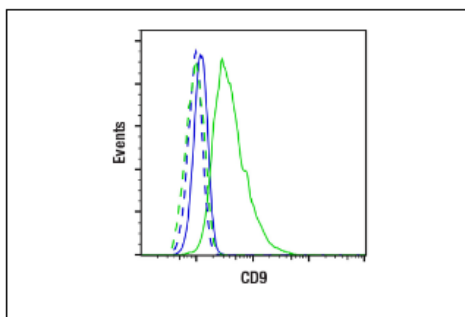
Western blot analysis of extracts from various cell lines using CD9 (E8L5J) Rabbit mAb (upper) and GAPDH (D16H11) XP® Rabbit mAb #5174 (lower). Absence of signal in BAF3 cells is predicted from RNAseq data and confirms the specificity of the antibody.



Confocal immunofluorescent analysis of RAW 264.7 cells (left, positive) or BAF3 cells (right, negative) using CD9 (E8L5J) Rabbit mAb (green) and DAPI #4083 (blue).

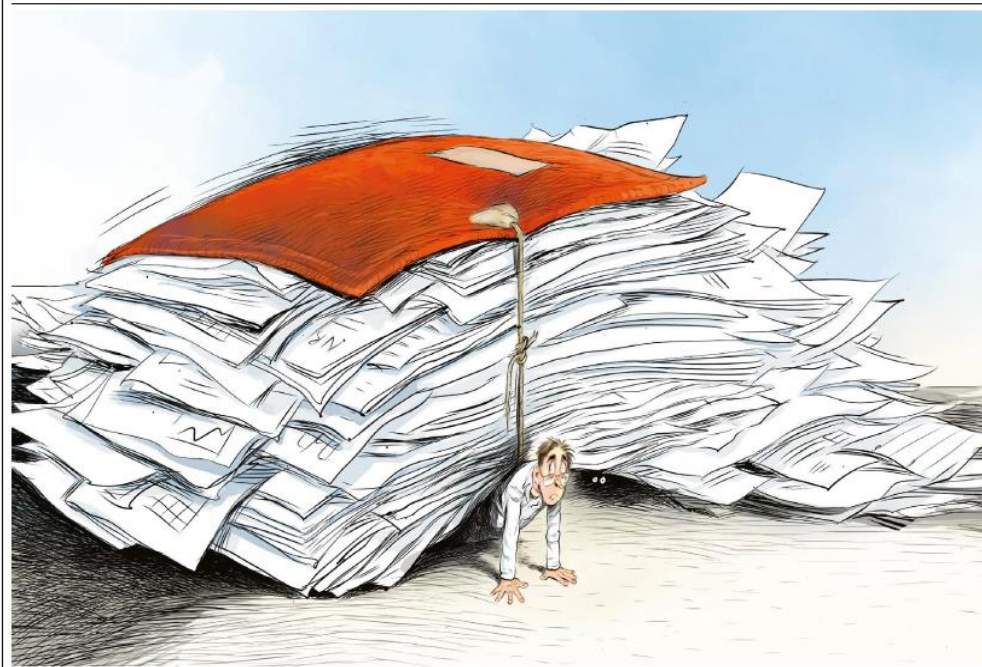


Flow cytometric analysis of live BAF3 cells (blue, negative) and JAWSII cells (green, positive) using CD9 (E8L5J) Rabbit mAb (solid lines) or concentration-matched Rabbit (DA1E) mAb IgG XP® Isotype Control #3900 (dashed lines). Anti-rabbit IgG (H+L), F(ab')₂ Fragment (Alexa Fluor® 488 Conjugate) #4412 was used as a secondary antibody.



Flow cytometric analysis of fixed and permeabilized BAF3 cells (blue, negative) and JAWSII cells (green, positive) using CD9 (E8L5J) Rabbit mAb (solid lines) or concentration-matched Rabbit (DA1E) mAb IgG XP® Isotype Control #3900 (dashed lines). Anti-rabbit IgG (H+L), F(ab')₂ Fragment (Alexa Fluor® 488 Conjugate) #4412 was used as a secondary antibody.

Comment



Reproducibility: expect less of the scientific paper

Olavo B. Amaral & Kleber Neves

Make science more reliable by placing the burden of replicability on the community, not on individual laboratories.

In 2018, we embarked on a journey to assess the reproducibility of biomedical research papers from Brazil. Thus began a multicentre collaboration of more than 60 laboratories to replicate 60 experiments from 2 decades of Brazilian publications¹. We randomly selected experiments that used three common laboratory techniques: the MIT assay for cell viability, RT-PCR to measure specific messenger RNAs and the elevated plus maze to assess anxiety in rodents.

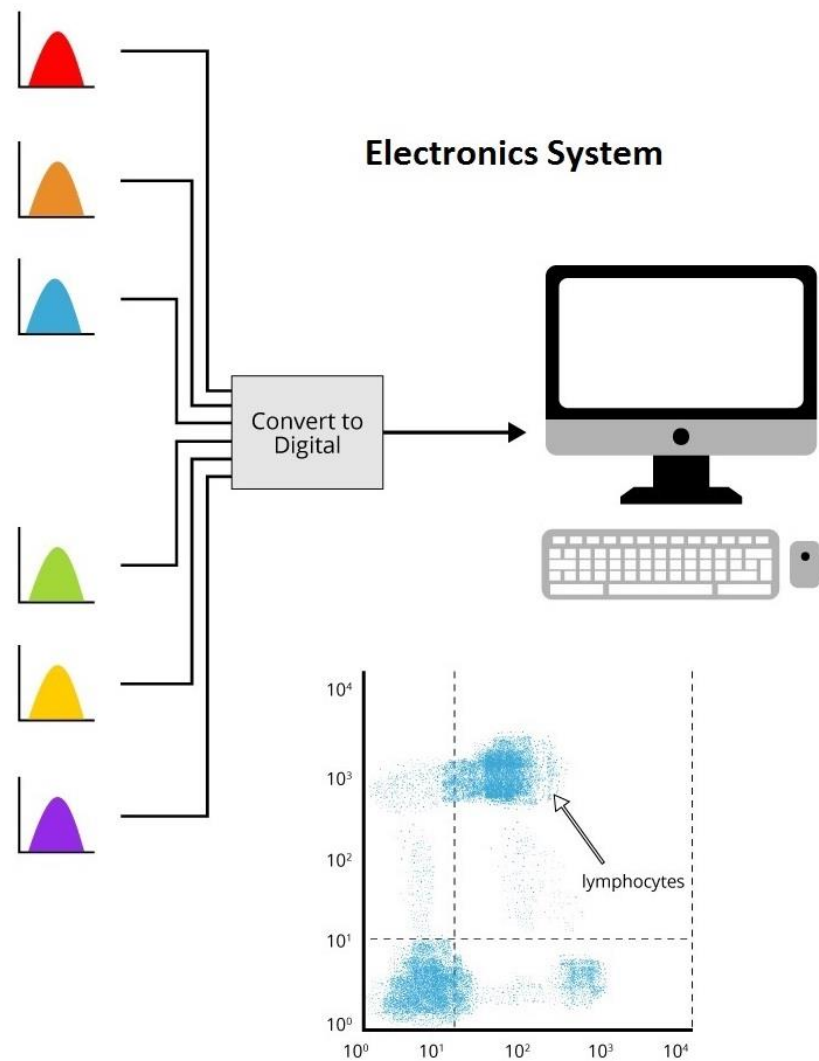
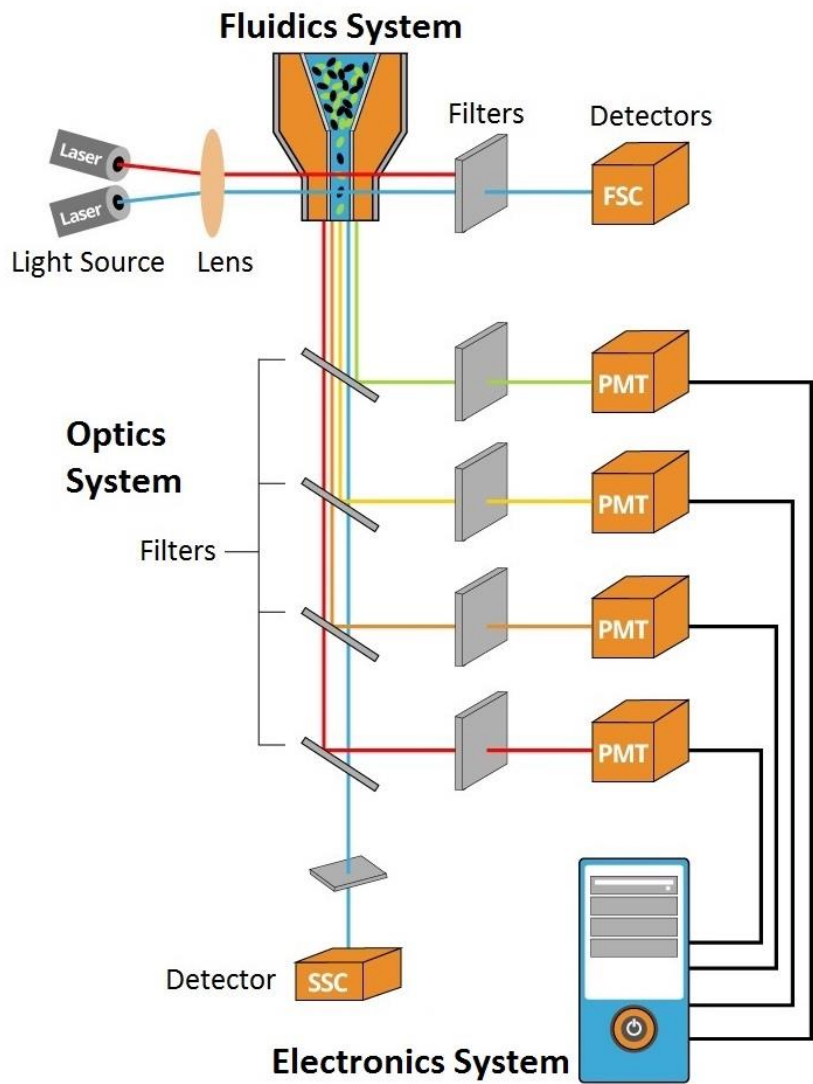
Each experiment will be repeated in three labs, and each lab has developed replication

protocols based on the original article's written methods. The process of building, reviewing and preregistering these protocols has taken months of communication between the coordinating team and the labs performing replications. We had intense arguments around the meaning of positive and negative controls and the merits of different metrics to define replication success. We also spent many hours on mundane tasks, such as studying the nutritional content of different brands of bologna sausage to better emulate a cafeteria diet fed to rats in one experiment.

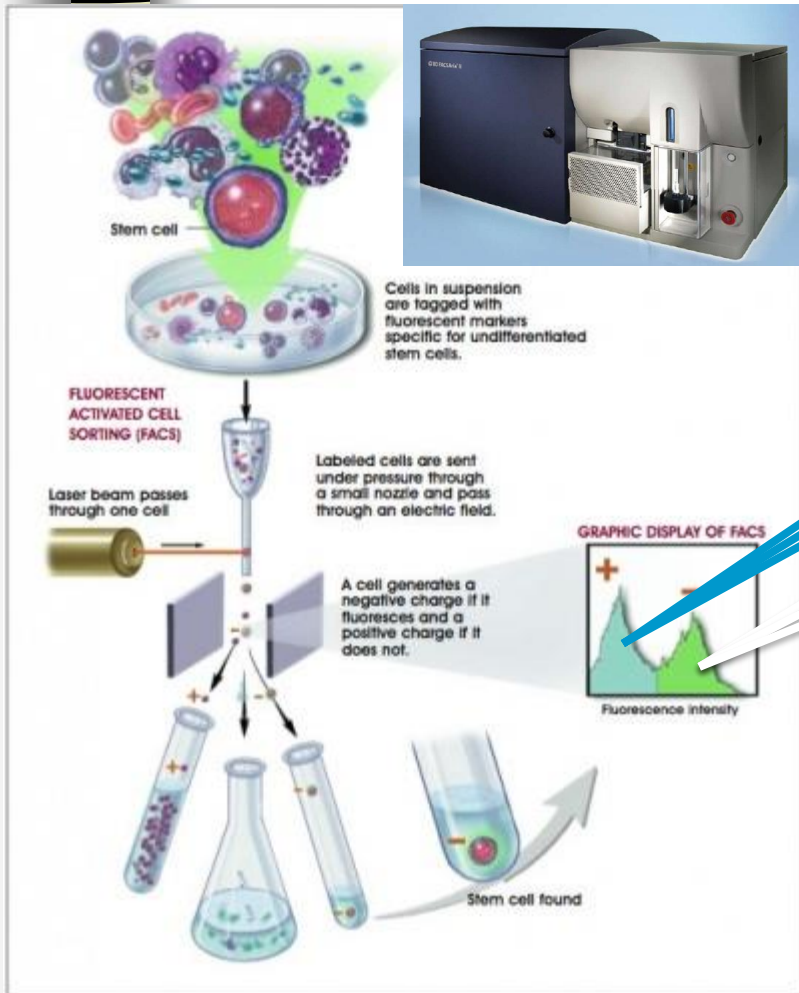
These are just some of the obstacles we

Dostupná technologie





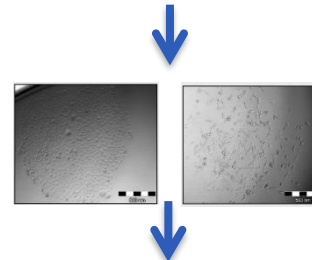
new automatic cell cloning assay (ACCA) for determination of clonogenic capacity of CSCs



single cell/well
up to 384 well plate



re-culture after sorting (2D, 3D)



analysis: CyQuant, ATP, xCelligence, microscopy





Principy průtokové cytometrie a sortování

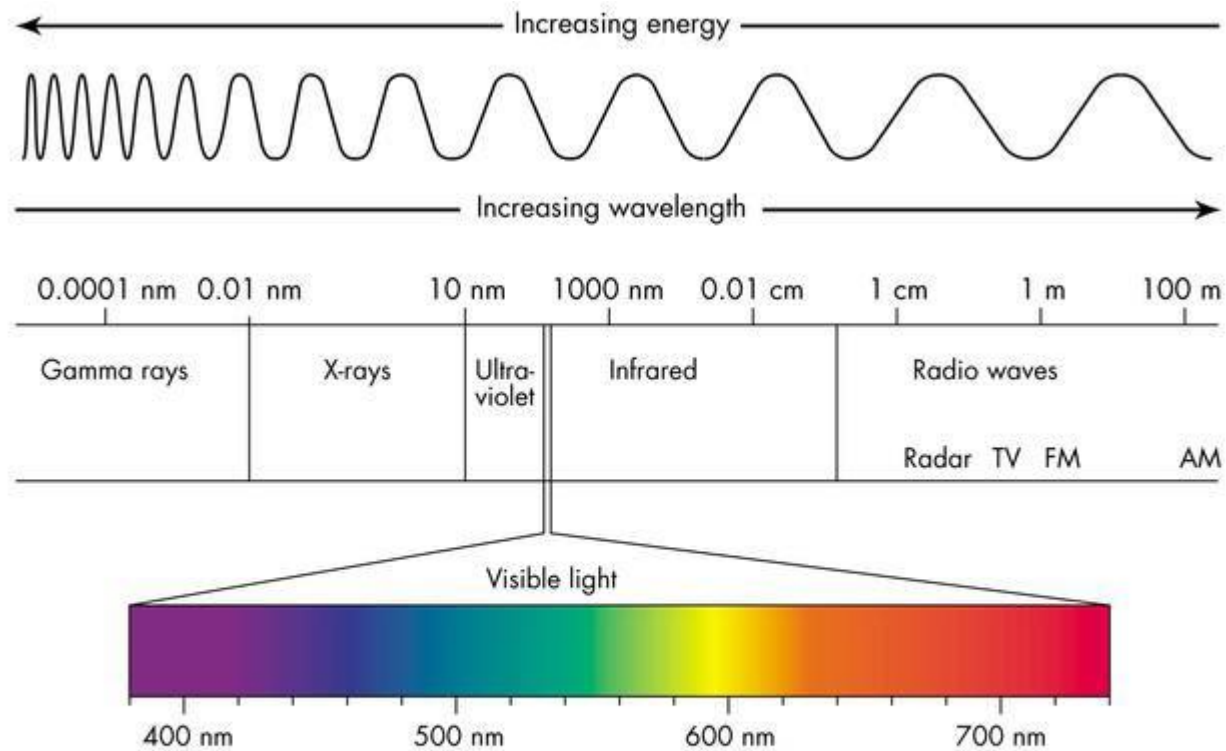
- Světlo
- Fluorescence
- Zdroje excitace, optické systémy a způsoby detekce fluorescence
- Fluidní systémy

Pojmy

Fotometrie:

- **Světlo** – elektromagnetické záření viditelné lidským okem (400-750 nm, nejcitlivější ~ 550 nm). Při měření pod 400 nm (UV, IF) se jedná detekci záření (radiometrie).
- Energie záření se vyjadřuje v *joulech*
- Světelný tok (**radiant flux**) je udávána jako hodnota energie v čase ve *wattech* (1 watt= 1 joule/sekundu)
- **foton** – elementární částice. Popisuje je jejich vlnová délka, frekvence, energie a hybnost. Životnost fotonu je nekonečná (přesto vznikají a zanikají), existují pouze v pohybu. Má nulovou klidovou hmotnost, ale nenulovou energii, definovanou vztahem $E = hv$, kde **h** je Planckova konstanta a **v** frekvence. Neboť má energii, působí na něj gravitace dle obecné teorie relativity a on sám gravitačně působí na okolí.
(<http://cs.wikipedia.org/wiki/Foton>)
- Energie fotonu je vyjádřena jako $E = hv$ a $E = hc/\lambda$ [**v**-frequency (Hz), **c** – rychlost světla (3×10^8 m/s), **λ**-wavelength (nm), **h**-Planckova konstanta (6.63×10^{-34} J/s)]
- **Energie** je vyšší při kratších vlnových délkách a nižší při delších vlnových délkách.

Elektromagnetické spektrum



Rozptyl světla

- Hmota rozptyluje světlo vlnových délek které není schopna absorbovat
- Viditelné spektrum je 350-850 nm proto malé částice a molekuly ($< 1/10 \lambda$) spíše viditelné světlo rozptylují
- Pro malé částice byl popsán tzv. **Rayleighův rozptyl (scatter)** jehož intenzita je \sim stejná všemi směry
- Rozptyl větších částic charakterizuje tzv. **Mieův rozptyl**. Jeho množství je větší ve směru v jakém dopadá světlo na ozářenou částici \Rightarrow *na tomto principu je založeno měření velikosti částic pomocí průtokového cytometru*



Rayleighův a Mieův rozptyl

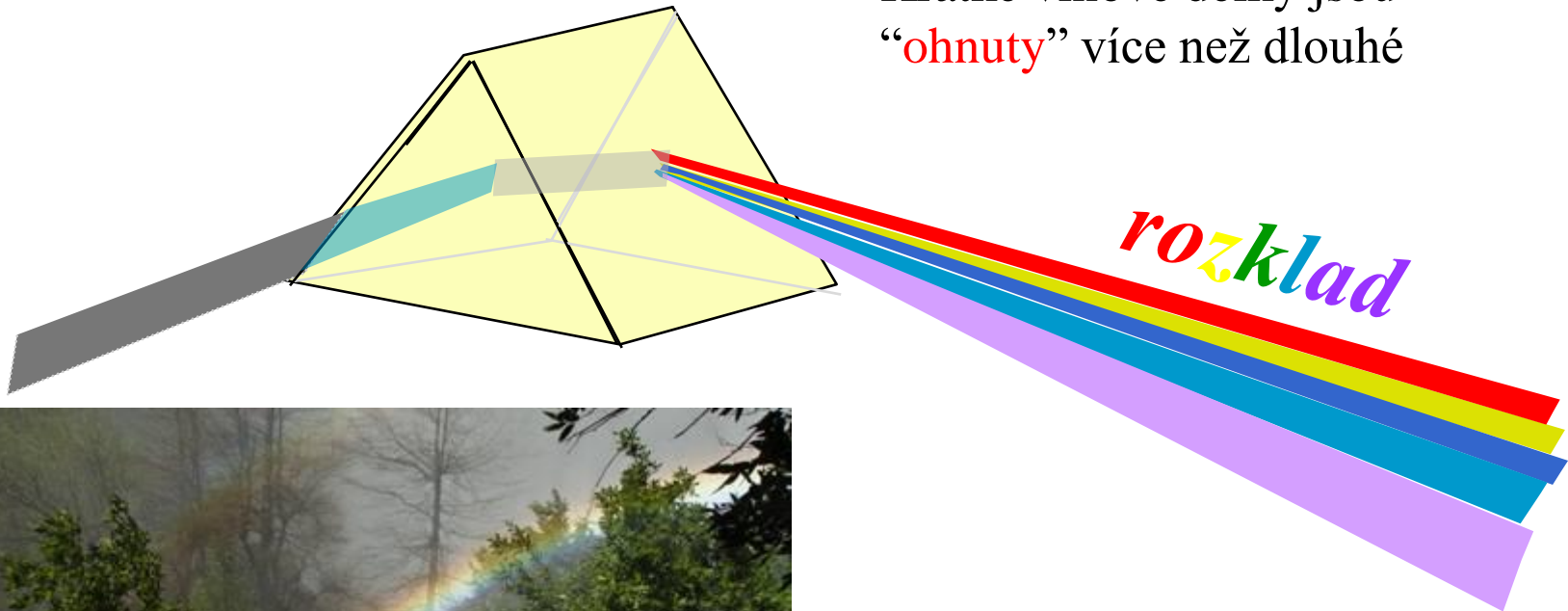
- **Rayleighův rozptyl** – molekuly a velmi malé částice neabsorbují, ale rozptylují světlo které má menší vlnovou délku než je jejich velikost (modré nebe - vzduch rozptyluje lépe kratší vlnové délky)
- **Mieův rozptyl** je charakteristický pro částice větší než je vlnová délka světla (bílá záře kolem slunečního kotouče, mlžné světlo)

<http://hyperphysics.phy-astr.gsu.edu/hbase/atmos/blusky.html>

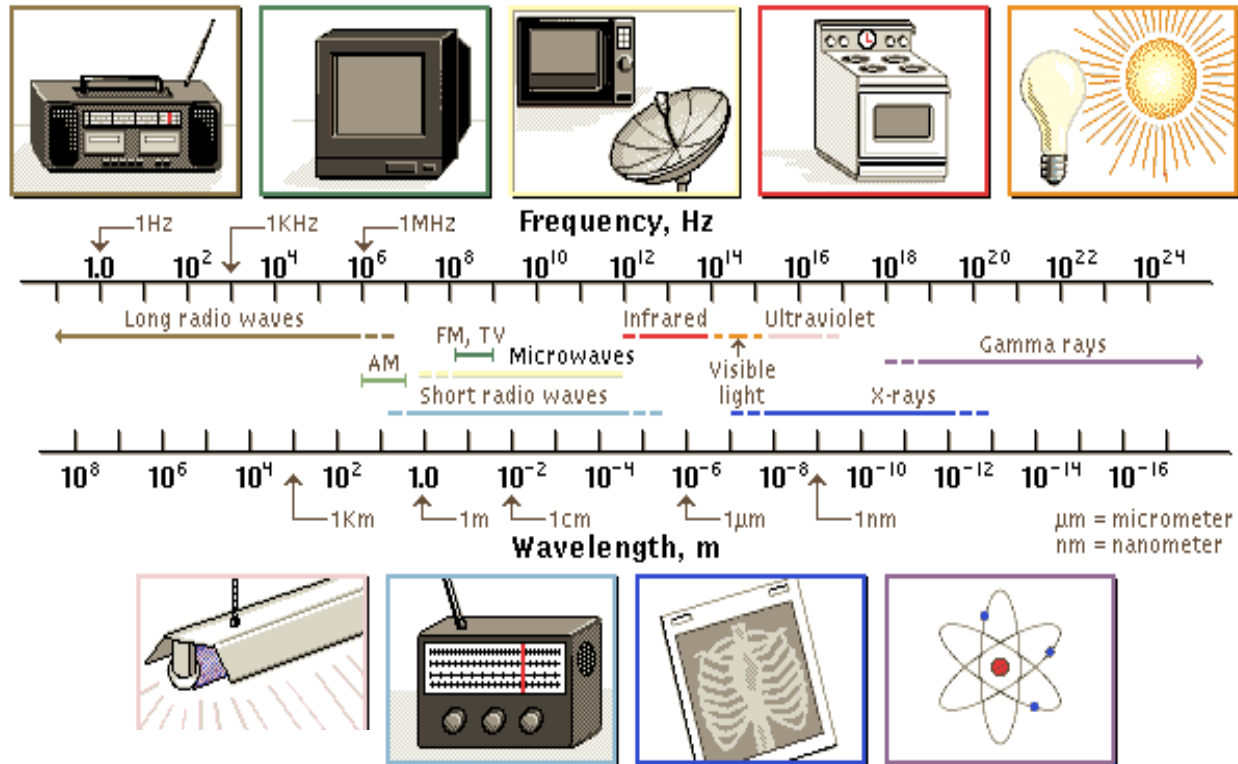


Ohyb a rozklad světla

Krátké vlnové délky jsou
“ohnuty” více než dlouhé



Elektromagnetické spektrum



© Microsoft Corp, 1995



Pouze malá oblast spektra je používána pro cytometrické aplikace

Fluorescence



George Gabriel Stokes (1819 – 1903)

Anglický fyzik a matematik
působící na univerzitě v Cambridge



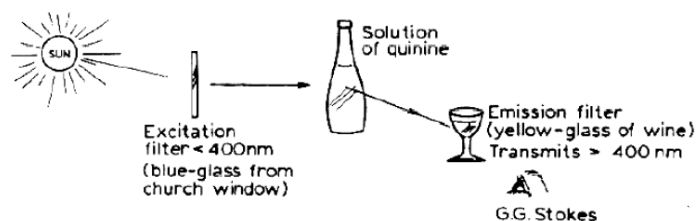
1852 – popsal fluorescenci

Název vznikl z anglického slova *fluospar*
(fluorit, kazivec = nerost CaF_2)

- ke svému pozorování použil roztok **chininu**,
jako zdroj světla sluneční paprsky, jako
excitační filtr sloužilo tmavě modré okenní
sklo a jako emisní filtr byla použita sklenice
bílého vína

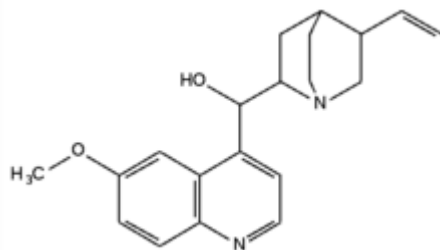


<http://www.nndb.com/people/131/000097837/>



G. C. Stokes „*On the Change of Refrangibility of Light*“ *Philosophical Transactions of the Royal Society of London*, 1852, vol. 142, p. 463.)

[463]

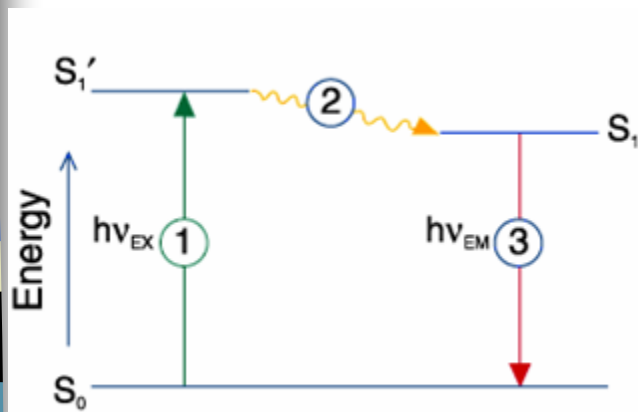


XXX. *On the Change of Refrangibility of Light.* By G. G. STOKES, M.A., F.R.S.,
Fellow of Pembroke College, and Lucasian Professor of Mathematics in the
University of Cambridge.

Received May 11,—Read May 27, 1852.

Princip fluorescence

Fluorescence (patří mezi fotoluminiscenční záření, které je vyvoláno buď účinkem jiného dopadajícího záření, nebo účinkem dopadajících částic) je výsledek tří fázového u jevu některých chemických látek - **fluorochromů**, fluorescenčních barev.



Jablonski diagram

Fáze 1: Excitace

- Záření z externího zdroje (např. laser) excituje fluorofor.
- Tím vzniká excitovaný stav (S_1').

Fáze 2: Životnost excitovaného stavu

- Excitovaný stav trvá krátkou dobu ($1-10^{-9}$ sekundy).
- Fluorofor může procházet změnami a interakcemi.
- Ztrácí část energie, vzniká uvolněný excitovaný stav (S_1).
- Některé molekuly nevrací energii formou fluorescenčního záření.
- To ovlivňuje fluorescenční kvantový výtěžek.

Fáze 3: Fluorescenční záření

- Fluorofor emituje foton a vrátí se do základního stavu (S_0).
- Energie emitovaného fotonu ($h\nu_{EM}$) je nižší a má delší vlnovou délku než excitační foton ($h\nu_{EX}$).
- Rozdíl se nazývá Stokesův posun a je klíčový pro citlivost fluorescenčních technik.



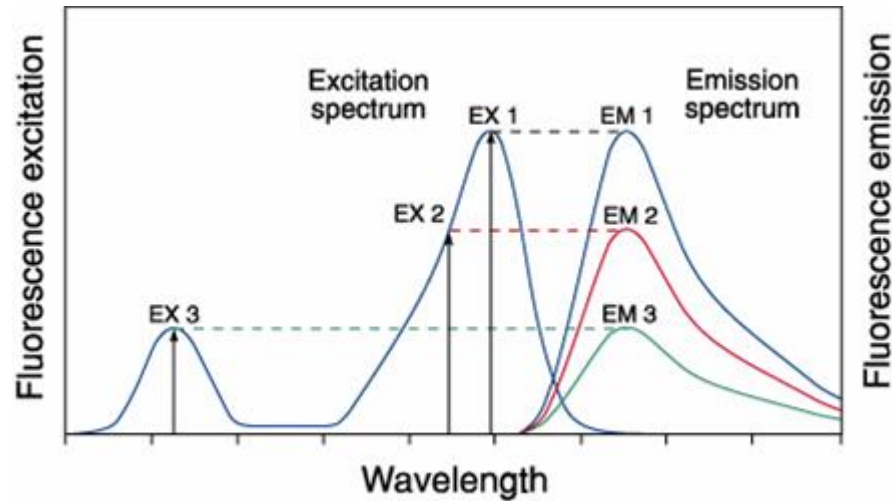
Charakteristiky fluorescence

- **intenzita** – počet fotonů procházejících v daném směru jednotkovou plochou za jednotku času
- **spektrální složení** – spektrální hustota fotonového toku na jednotkový interval vlnových délek nebo frekvencí
- **polarizace** – směr kmitání elektrického vektoru elektromagnetické vlny
- **doba dohasínání** – je dána vnitřní dobou života excitovaného stavu, z něhož dochází k emisi; úzce souvisí s pochody vedoucími k nezářivé deaktivaci tohoto stavu
- **koherenční vlastnosti** – vztahy mezi fázemi světelných vln

Fluorescenční spektra

Fluorescenční proces je cyklický.

Kromě fluorochromu nevratně zničeného (photobleaching - „vysvícení“) může být opakovaně excitován.



Excitation of a fluorophore at three different wavelengths (EX 1, EX 2, EX 3) does not change the emission profile but does produce variations in fluorescence emission intensity (EM 1, EM 2, EM 3) that correspond to the amplitude of the excitation spectrum.



Fluorescenční barviva

- Fluorescenční barviva (fluorofory, fluorochromy) jsou chemické sloučeniny, které obsahují ve své molekule reaktivní skupinu, která je schopna reagovat s nukleofilními skupinami (NH_2 , OH , SH).
- Obecně se fluorofory dělí na vnitřní (vlastní, intrinsic) a vnější (nevlastní, extrinsic).

Vnitřní fluorescence

- Vnitřní fluorescence buněk je dána přítomností vnitřních fluoroforů, mezi které patří proteiny, redukované formy NADH a NADPH, vitamin A, cytochromy, peroxidáza, hemoglobin, myoglobin či chlorofyl.
- Proteiny vyzařují fluorescenční záření v UV oblasti spektra. Hlavními fluorofory v proteinech jsou aromatické aminokyseliny (fenylalanin, tryptofan, tyrosin), jejichž absorpční i emisní pás leží mezi 240 a 300nm.
- Ostatní uvedené látky vyzařují ve viditelné oblasti spektra (modrá, žlutá či červená).

Vnější fluorescence

- Vnější fluorofory jsou používány mnohem častěji než vnitřní.
- Jsou přidávány ke studovanému vzorku a podle typu vazby jsou děleny na fluorescenční značky a fluorescenční sondy.

Fluorescenční značky

- Nejčastěji se používají k fluorescenčnímu značení proteinů, ke kterým se vážou kovalentní vazbou.
- Nejznámějšími fluorescenčními značkami jsou FITC (fluorescein-5-isothiokyanát) a TRITC (tetramethylrhodamin-5-isothiokyanát, tetramethylrhodamin-5-isothiokyanát).

Fluorescenční sondy

- vnější fluorofory, které se váží ke struktuře nekovalentní vazbou a často při tom mění své fluorescenční vlastnosti. Tyto fluorofory jsou používány ke studiu změn konformace bílkovin, tloušťky membrán, membránového potenciálu apod.
- K identifikaci a vizualizaci nukleových kyselin se používá řada fluorescenčních sond (např: akridinová oranž, ethidium bromid, DAPI a další).
- Nejznámější a také nejpoužívanější fluorescenční sondou pro vizualizaci veškeré jaderné DNA je DAPI. Chemicky se jedná o 4',6-Diamidino-2-fenylindol. Jeho absorpční maximum je při 345 nm, maximální fluorescence je při 455 nm (modrý fluorofor)
- Dalším často používaným fluoroforem je akridinová oranž. Jedná se o fluorescenční sondu, jejíž absorpční a emisní pásma se liší podle substrátu, ke kterému je vázána DNA/RNA. Obě jmenované jsou většinou dodávány v podobě chloridových solí.

Detekce fluorescence

Vybavení pro fluorescenci

- (1) zdroj excitace
- (2) fluorochrom
- (3) vlnové filtry pro izolaci emitovaných fotonů od excitovaných
- (4) detektory pro registraci emitovaných fotonů

Fluorescenční přístroje

- spektrofluorometer měří průměrné vlastnosti objemu vzorku v kyvetě.
- fluorescenční mikroskop popisuje fluorescenci jako jev v prostorovém systému souřadnic
- flow cytometr měří fluorescenci v proudícím toku, umožňuje detekovat a kvantifikovat subpopulace uvnitř velkého vzorku

Fluorescenční signál

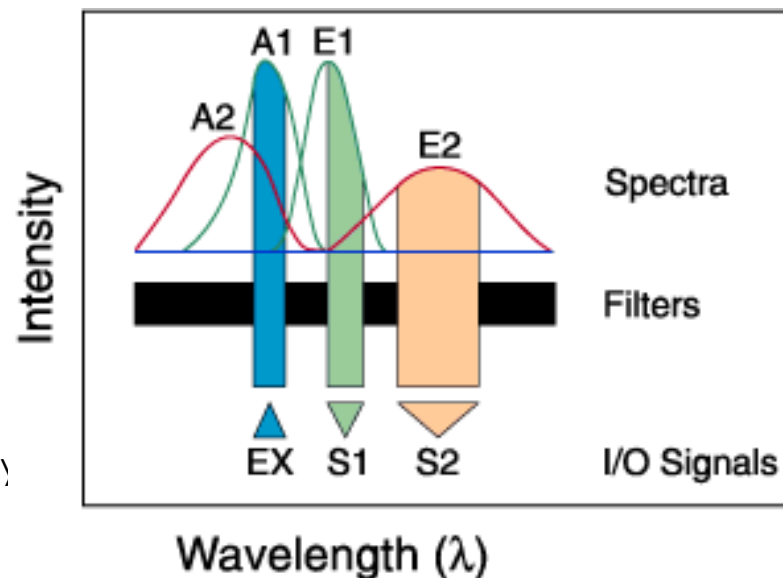
- spektrofluorometer je flexibilní, umožňuje měřit v kontinuálním spektru excitačních a emisních vlnových délek
- flow cytometr potřebuje fluorescenční značky excitovatelné určitou vlnovou délkou.

Fluorescence pozadí

- endogenní složky - autofluorescence
- nenávanané nebo nespecificky vázané značky = reagenční pozadí

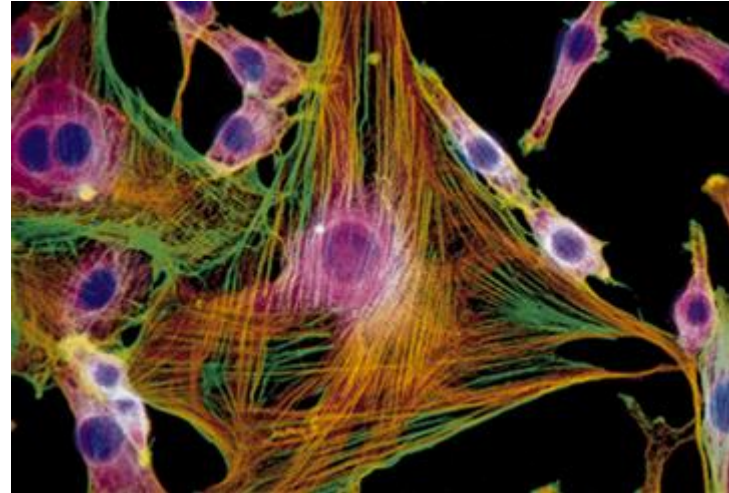
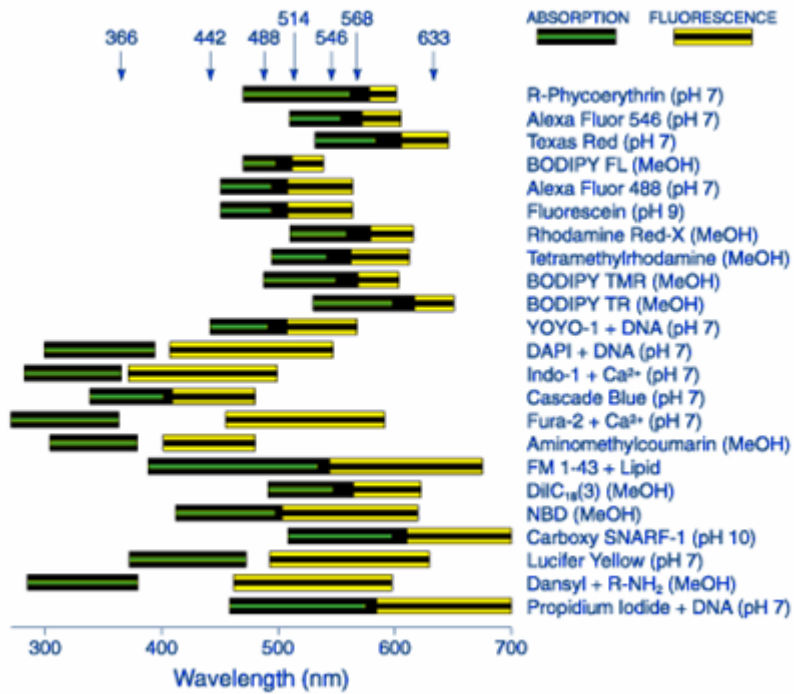
Vícebarevné značení

- dvě a více značek, zároveň monitoruje různé funkce
- nutné: vhodně zvolit značky zdroj excitace a separační filtry



Fluorescence Output of Fluorophores

Comparing Different Dyes



Mouse 3T3

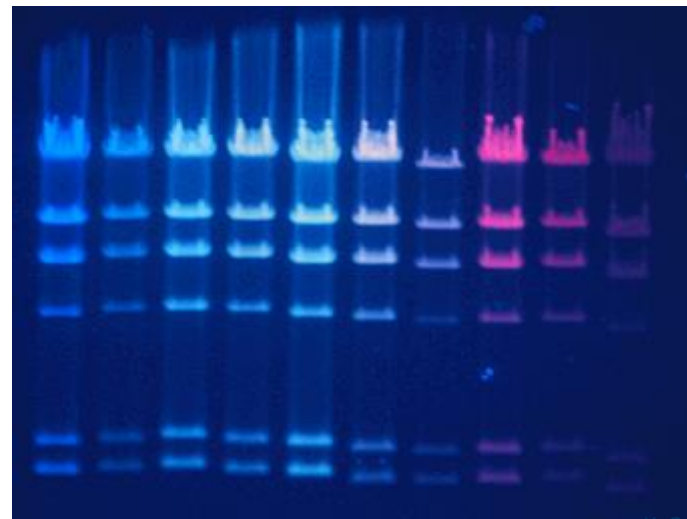
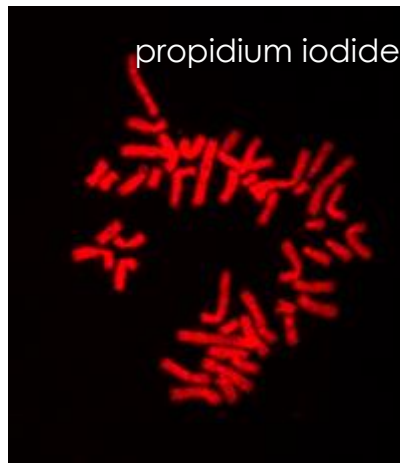
F-actin ~
BODIPY FL phalloidin

anti-β tubulin ~
Texas Red
goat anti-mouse IgG

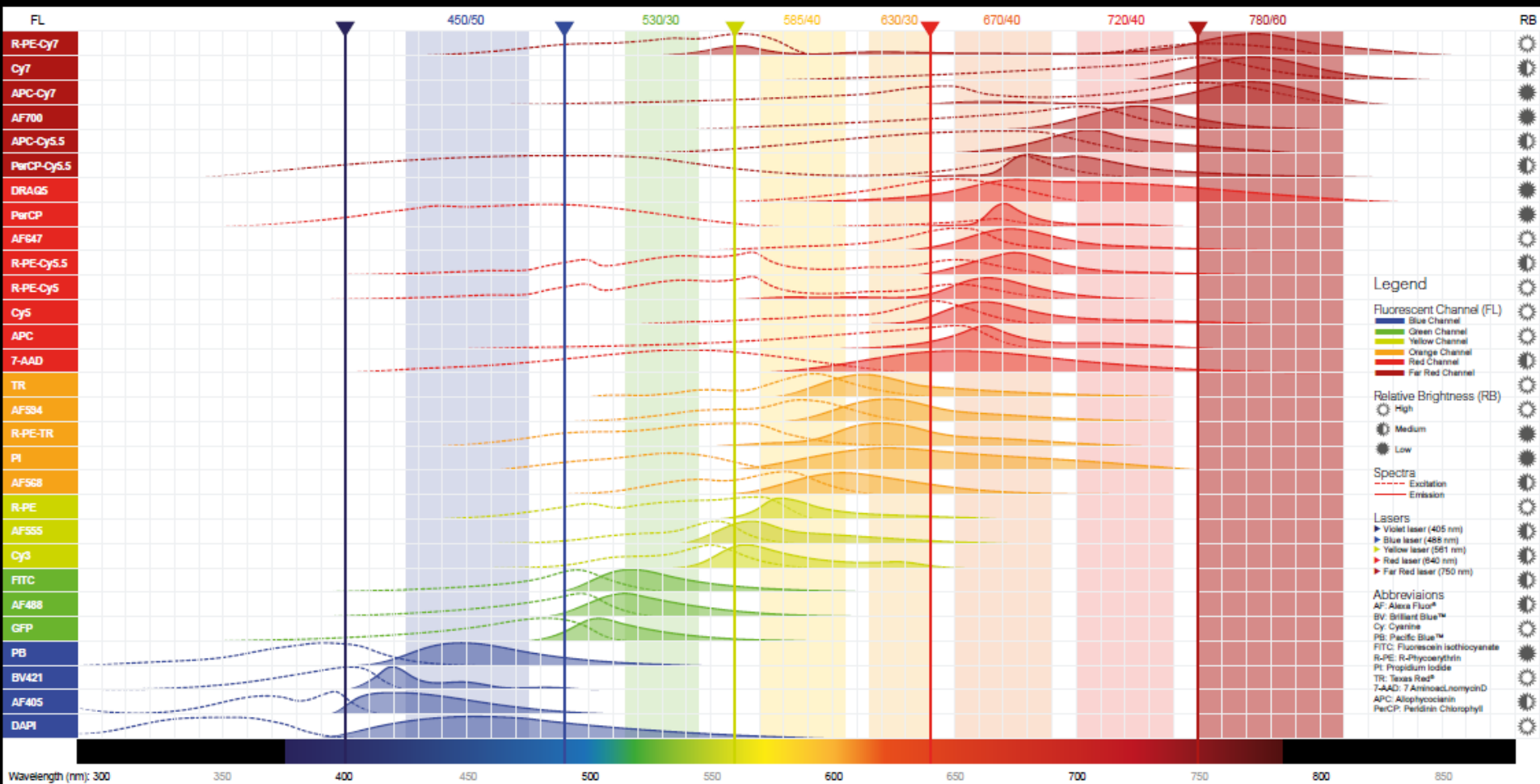
DNA ~
DAPI

POPO-1 BOBO-1 YOYO-1 TOTO-1 JOJO-1 POPO-3 LOLO-1 BOBO-3 YOYO-3 TOTO-3

λ Hind III



Fluorochrome chart



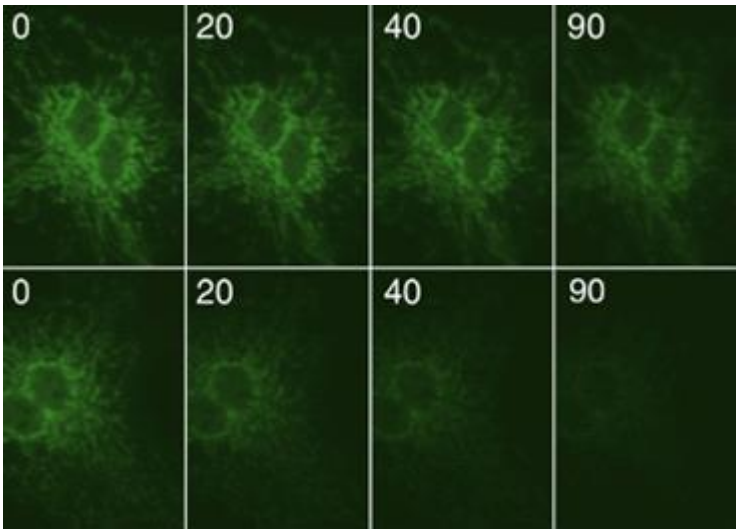


Procesy interferující a detekcí fluorescence

- **Quenching** - „zhášení“ fluorescence pomocí polárních rozpouštědel, těžkých iontů.
- **Bleaching** – změna struktury fluorescenční molekuly vedoucí ke ztrátě fluorescence (působením světla a nebo chemickou interakcí).
- **Photon saturation** – stav kdy množství molekul v excitovaném stavu odpovídá množství molekul v bazální hladině

Photobleaching

- irreversible destruction or photobleaching of the excited fluorophore



anti-human cytochrome oxidase subunit I

Oregon Green 514 goat anti-mouse IgG

fluorescein goat anti-mouse IgG

Základ průtokové cytometrie



Fluidics

Optics

Electronics

Buňky v suspenzi

protékají jednotlivě napříč

osvětlenou částí kde

rozptylují světlo a emitují
fluorescenci,

která je detekována, filtrována a

převedená na digitální hodnoty

uložené do počítače



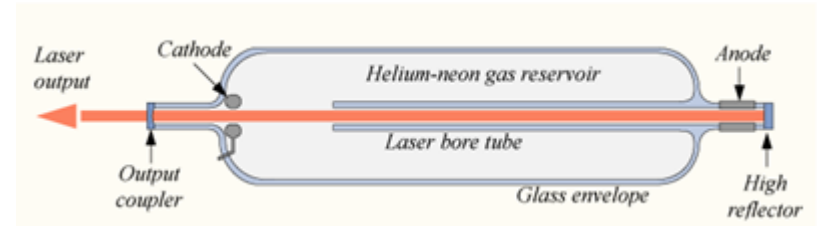
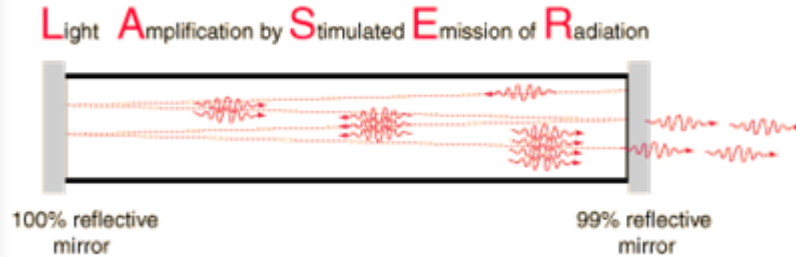
Optika - zdroj světla

- nutnost zaostřit zdroj světla na stejné místo, kde je zaostřen průtok buněk
- Lasery
 - produkují jednotlivou vlnovou délku světla (325, 488, ~630nm)
 - poskytují mW - W světla
 - poskytují koherentní světelný proud
- Obloukové lampy (Arc-lamps), s současných systémech je již nenajdeme
 - produkují **směs** vlnových délek, které musí být filtrovány
 - poskytují mW světla
 - levné - air-cooled
 - nekoherentní světelný proud

- optické kanály

- cesta světla z místa ozáření buněk k detektoru
- optické části **separují** určité vlnové délky

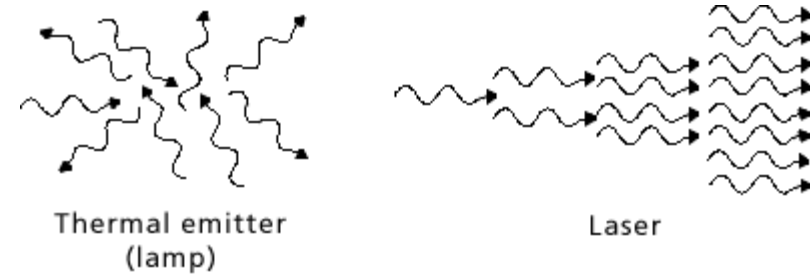
LASER(y)



http://en.wikipedia.org/wiki/Helium-neon_laser

- koherentní (souvislý světelný tok)
- monochromatický
- soustředěný

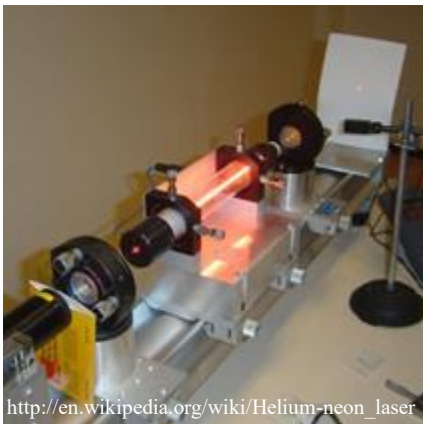
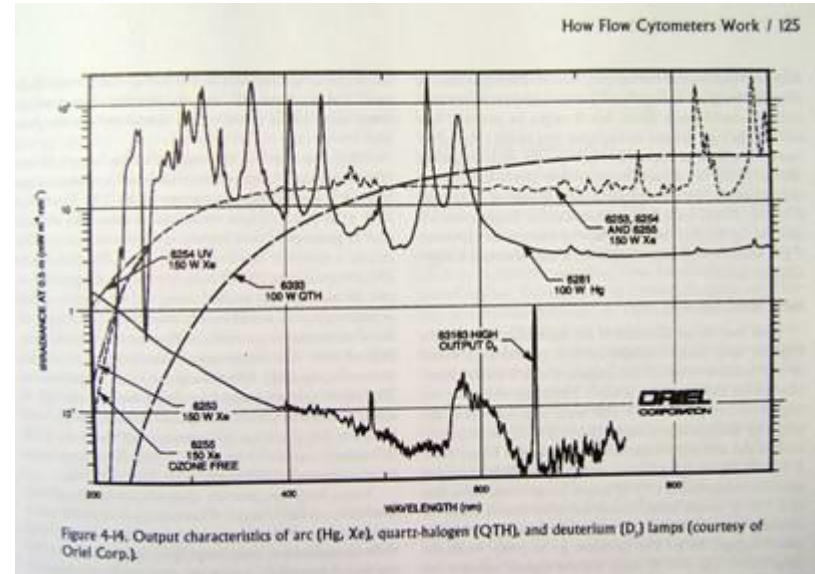
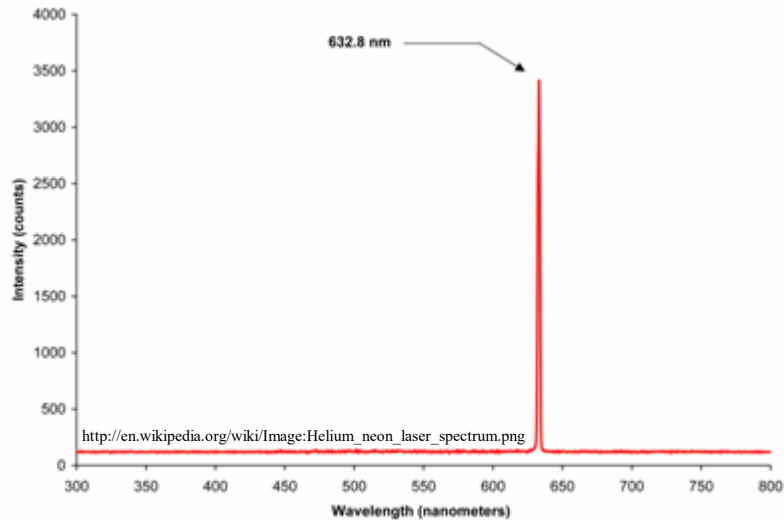
<http://hyperphysics.phy-astr.gsu.edu/hbase/hframe.html>



<http://www.ilt.fraunhofer.de/eng/100053.html>



LASER vs. Arc lamp



H.M. Shapiro, Practical Flow Cytometry, 4th ed.



<http://www.olympusmicro.com/primer/anatomy/sources.html>

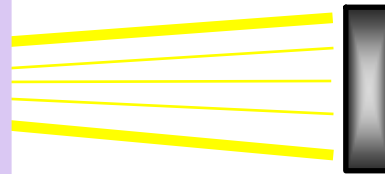
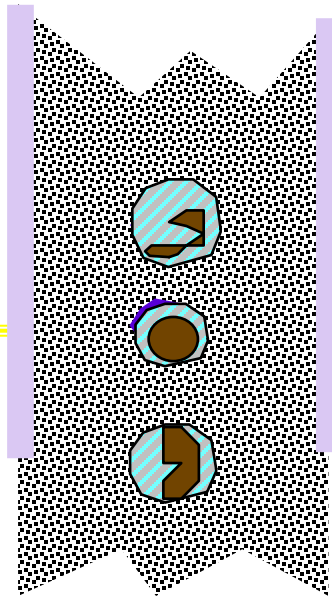
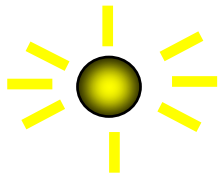


Optika - „Forward Scatter“ kanál

- část světla rozptýlená ve stejné ose jako je směr světelného paprsku
- intenzita „forward scatteru“ odpovídá velikosti, tvaru a optické homogenitě buněk

Forward Angle Light Scatter

Laser



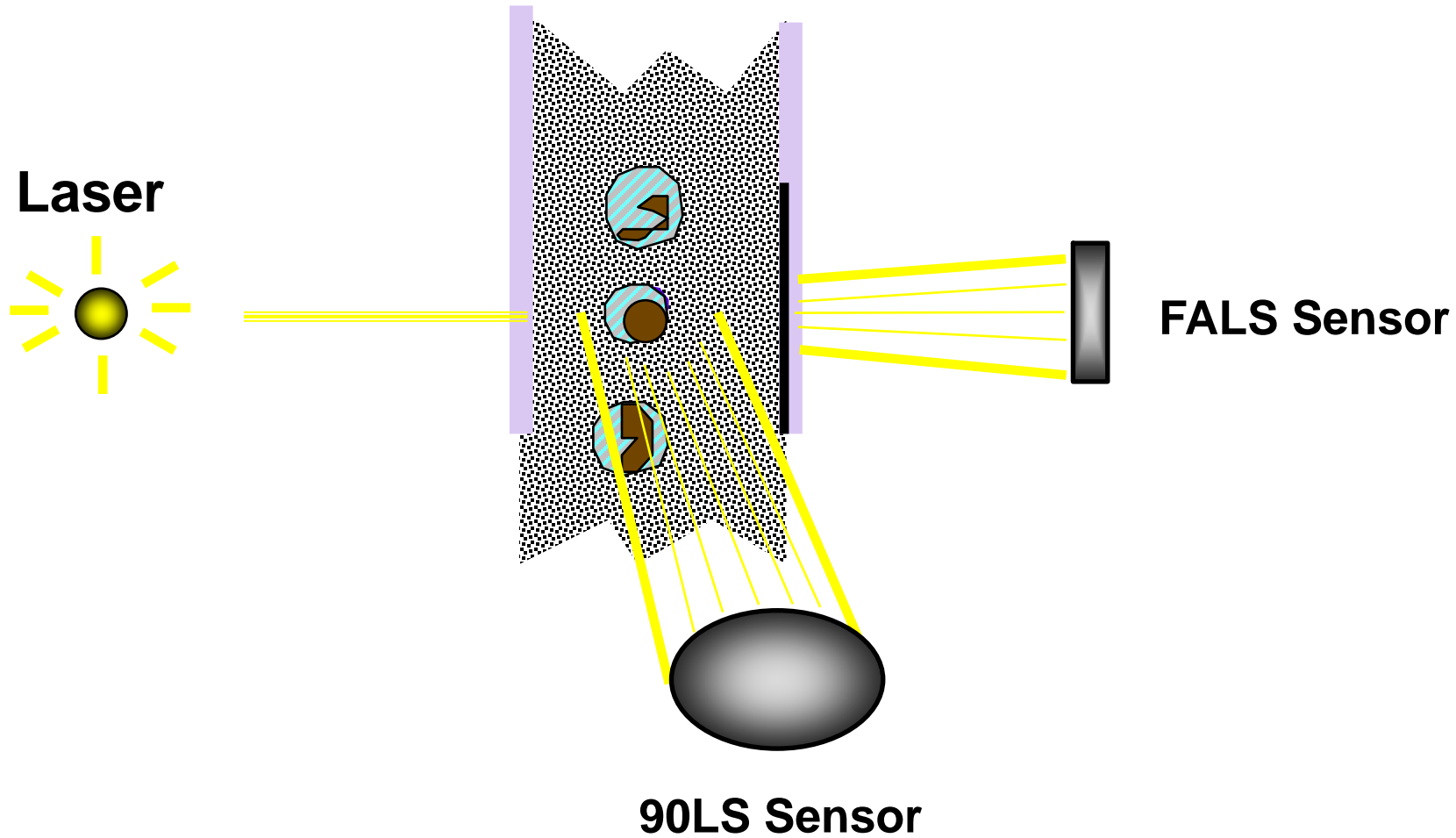
FALS
Sensor



Optika - „Side Scatter“ kanál

- část světla rozptýlená kolmo do strany od osy směru světelného paprsku **side (90°) scatter channel**
- intenzita „side scatteru“ odpovídá **velikosti, tvaru a optické homogenitě** buněk

90 Degree Light Scatter





Optika - Light Scatter

- „Forward scatter“ zachycuje **povrchové vlastnosti a velikost** částic
- může být použit k rozlišení živých a mrtvých buněk
- „Side scatter“ odpovídá **inkluzím uvnitř** buněk
 - možno odlišit **granulární** a **negrnulární** populaci

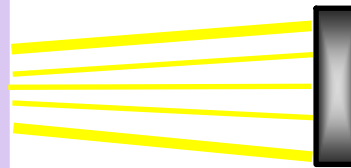
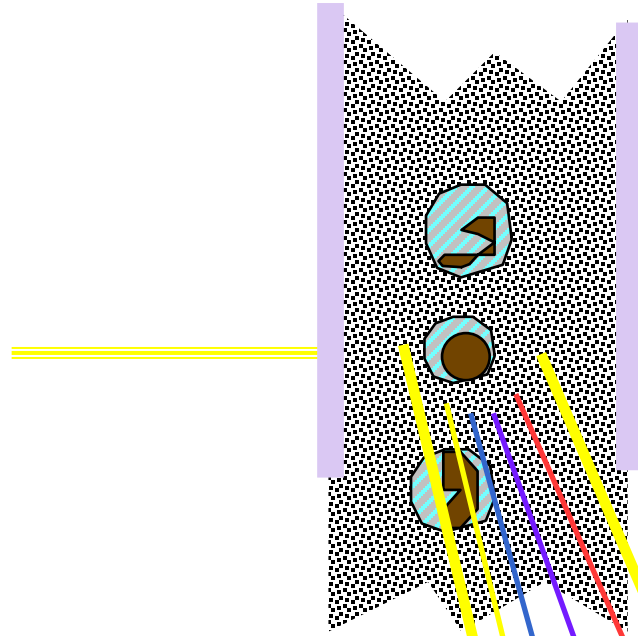
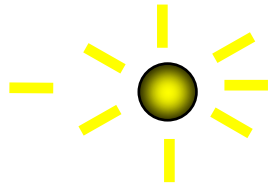


Optika - fluorescenční kanály

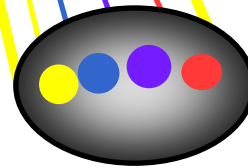
- fluorescence emitovaná z každého fluorochromu je detekována pomocí specifického **fluorescenčního kanálu**
- specifita detekce je kontrolována vlnovou selektivitou filtru a zrcadel

Fluorescence Detectors

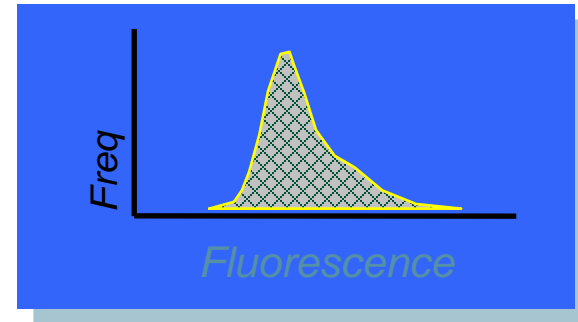
Laser



FALS Sensor



Fluorescence detector
(PMT3, PMT4 etc.)



Optika - vlastnosti filtrů

- jsou konstruovány z materiálů absorbujících určitou vlnovou délku (a propouštějí jinou)
- přechod mezi absorbancí a transmisí není přesný; nutné specifikovat lom světla při konstrukci filtru

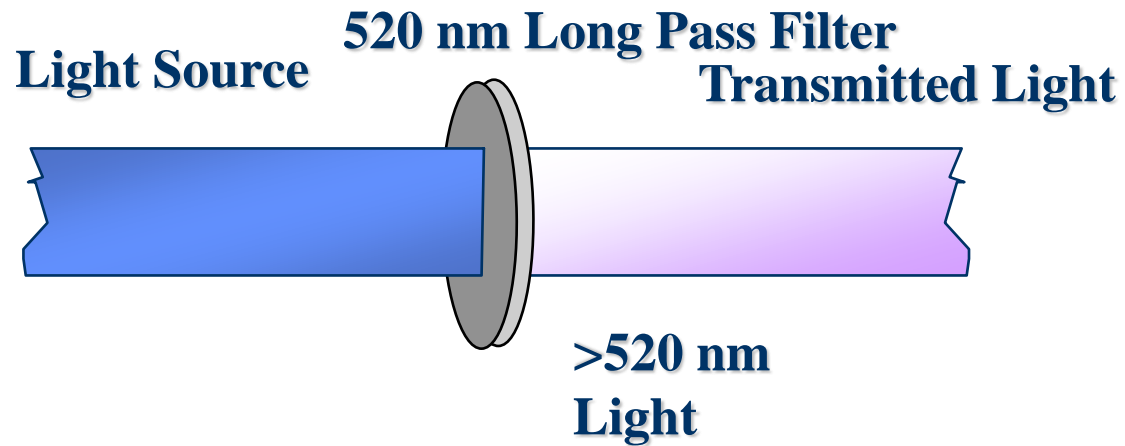




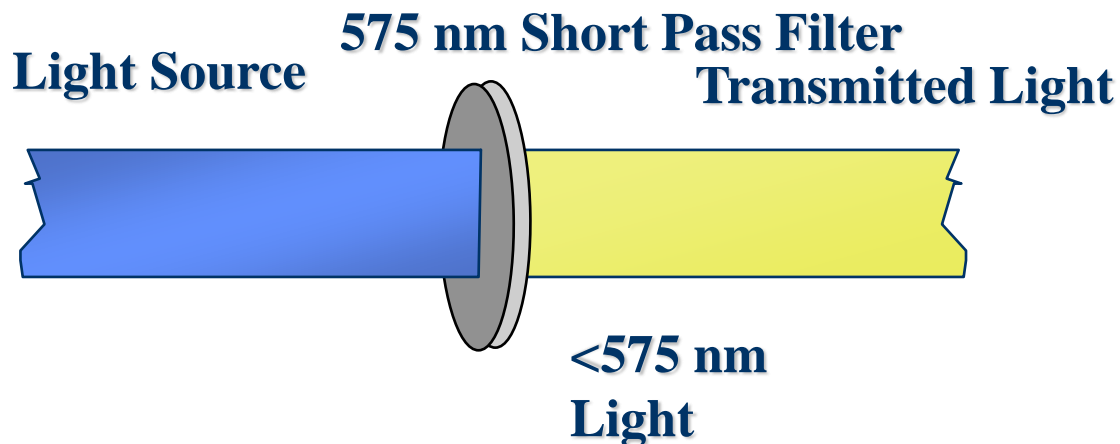
Optics - vlastnosti filtrů

- „Long pass“ filtr propouští vlnovou délku **nad** „řezanou“ délkou
- „Short pass“ filtr propouští vlnovou délku **pod** „řezanou“ délkou
- „Band pass“ filtr propouští vlnovou délku v **úzkém rozmezí** okolo specifické vlnové délky

Standard Long Pass Filters



Standard Short Pass Filters

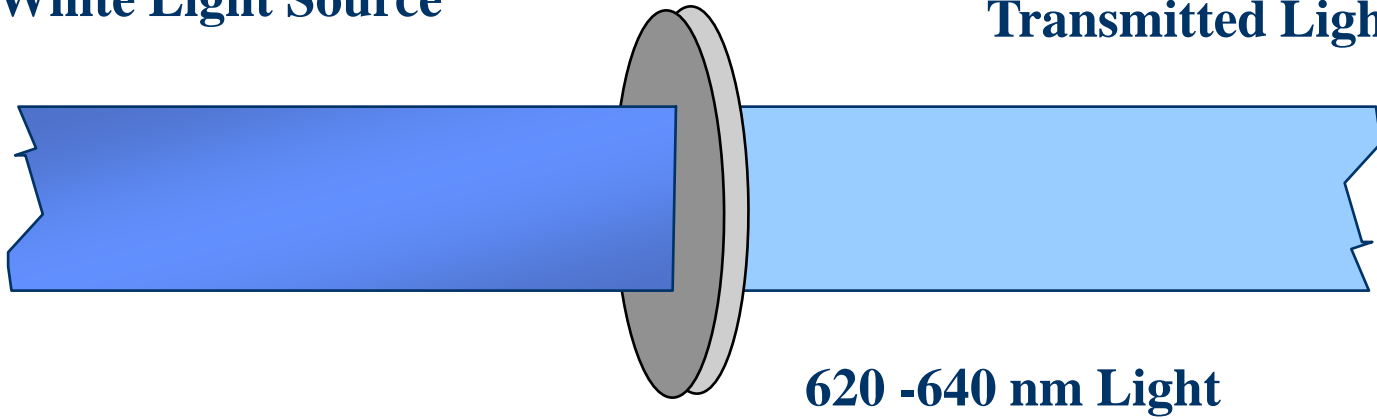


Standard Band Pass Filters

630 nm BandPass Filter

White Light Source

Transmitted Light





Optika - vlastnosti filtrů

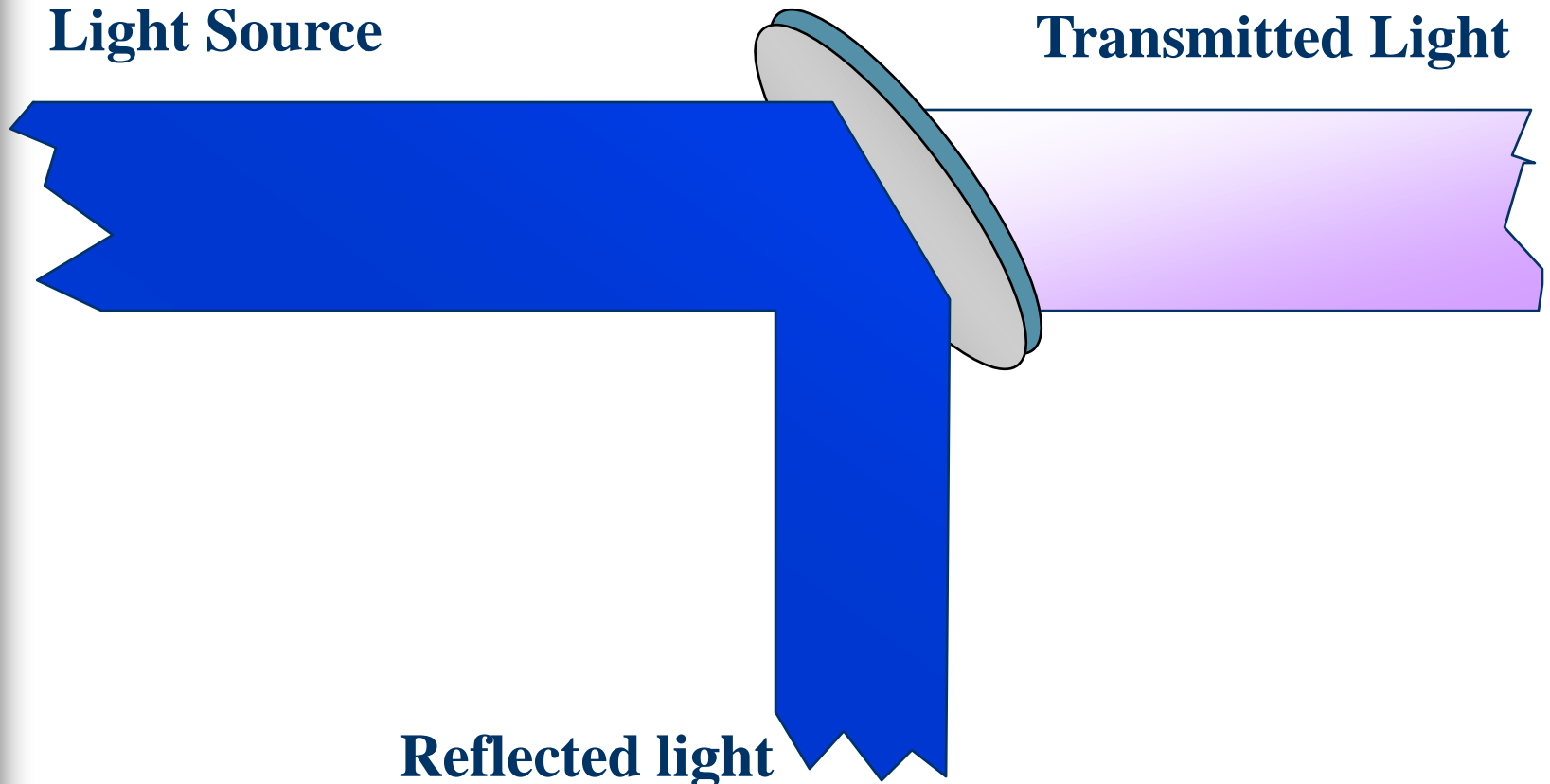
- pokud je filtr umístěn v **45° úhlu** ke zdroji světla, světlo, které má projít tak projde, ale blokované světlo je odraženo v 90° úhlu
- **dichroické filtry, dichroická zrcadla**

Dichroic Filter/Mirror

Filter placed at 45°

Light Source

Transmitted Light



Reflected light



Optika - uspořádání filtrů

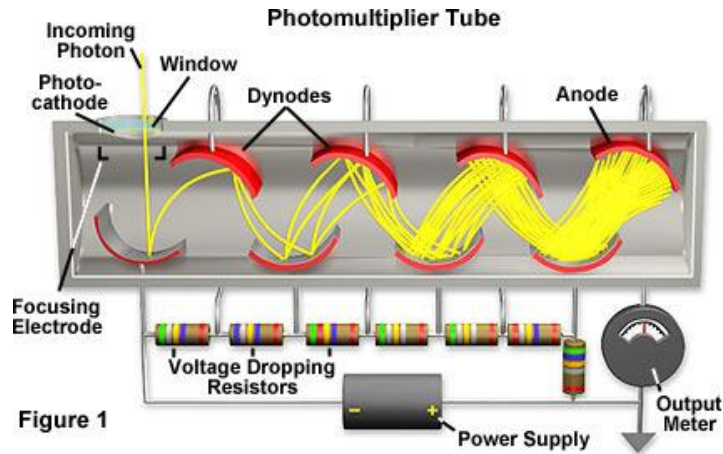
- k společnému měření více než jednoho „scatteru“ nebo fluorescence , používáme **mnohonásobné kanály** (a detektory)
- multikanálové uspořádání musí splňovat
 - **spektrální vlastnosti** použitého fluorochromu
 - **správný řád uspořádání** filtrů a zrcadel



Optika - detektory

- dva obecné typy detektorů
 - **fotodioda**
 - v minulosti zejména pro silný signál (forward scatter detector)
 - současnost – vysoce citlivé AVALANCHE“ fotodiody (APD)
 - **fotonásobič (photomultiplier tube - PMT)**
 - citlivější než běžná fotodioda, může být poškozen přesvícením

Photomultiplier tubes (photomultipliers, PMTs)



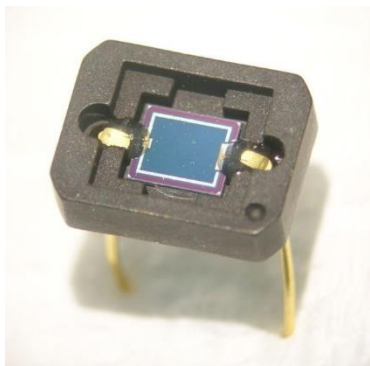
Základní charakteristika:

- vysoce citlivé detektory (jeden foton)
- velké zesílení signálu/nízký šum
- velká plocha detekce
- rychlá frekvence odpovědi
- velké pracovní napětí (1000 – 2000 V)

<http://en.wikipedia.org/wiki/Photomultiplier>

<http://hamamatsu.magnet.fsu.edu/articles/photomultipliers.html>





<http://en.wikipedia.org/wiki/Photodiode>

“bežná“ fotodioda

Porovnání s PMT

Výhody:

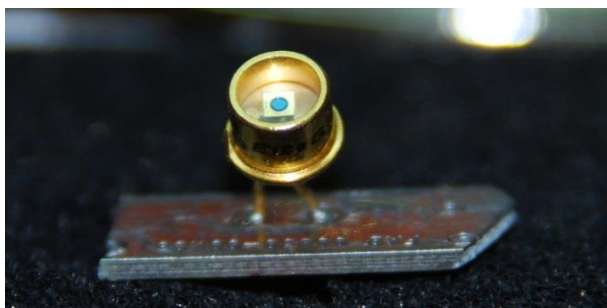
1. excelentní linearita signálu
2. rozsah spektrální detekce 190 nm to 1100 nm (silicon)
3. nízký šum
4. Odolnost vůči mechanickým vlivům
5. nízká cena
6. malá velikost a hmotnost
7. dlouhá životnost
8. Vysoká kvantová účinnost (~80%)
9. Nepotřebuje vysoká napětí

Nevýhody

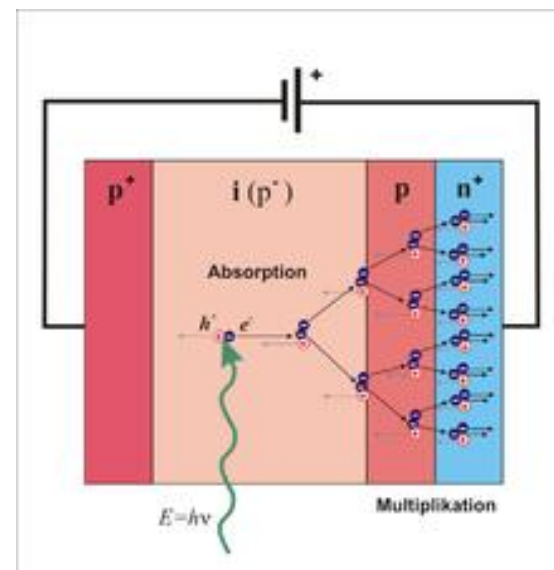
1. Malá plocha
2. Nemožnost integrálního zesílení
3. Mnohem nižší citlivost
4. Počítání fotonů pouze u speciálních produktů
5. Kratší čas odpovědi

Současnost: „AVALANCHE“ fotodiody (APD)

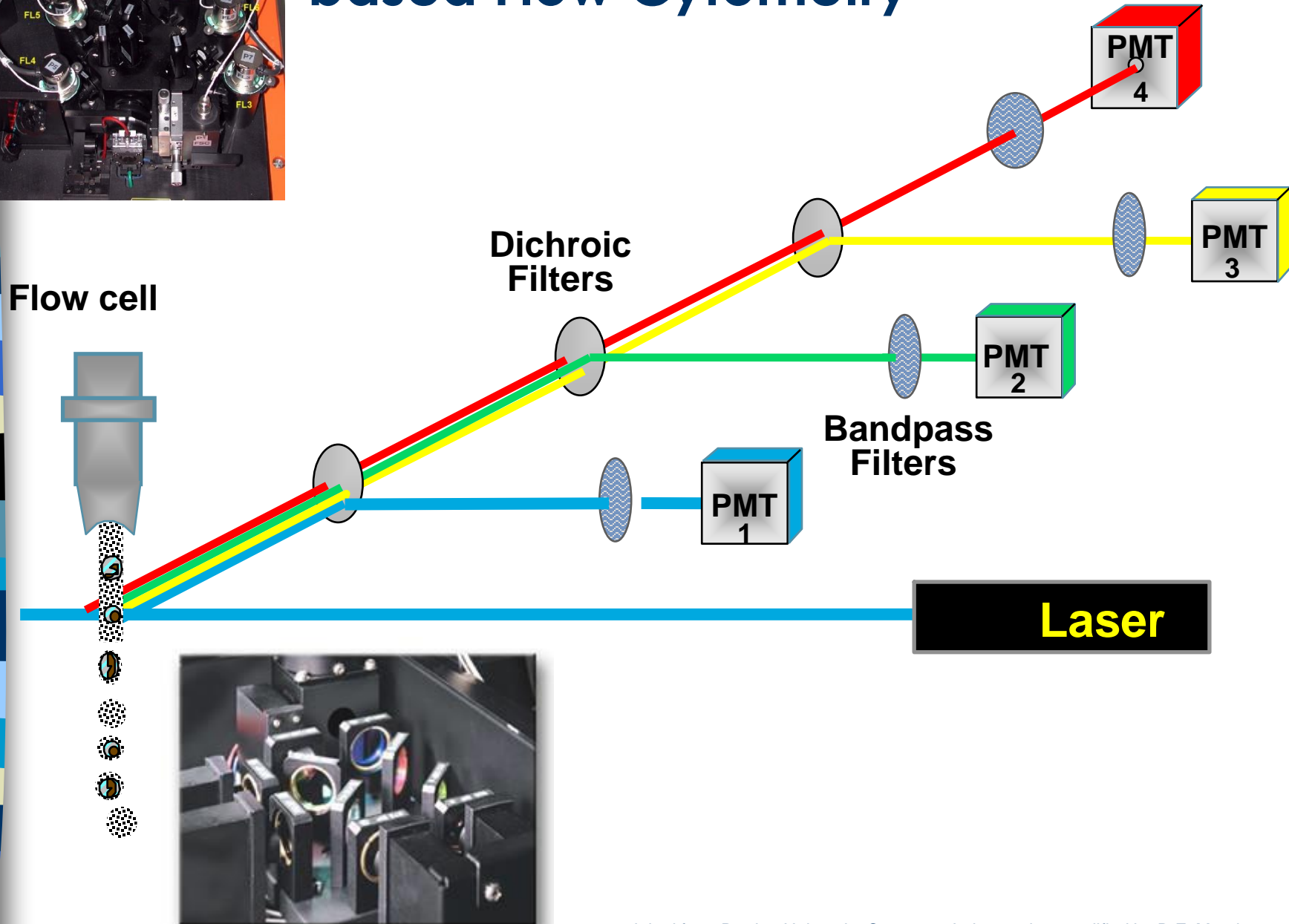
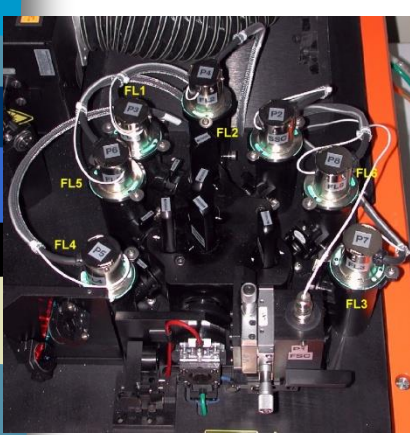
- Vysoce citlivé polovodiče - srovnatelné s PMT



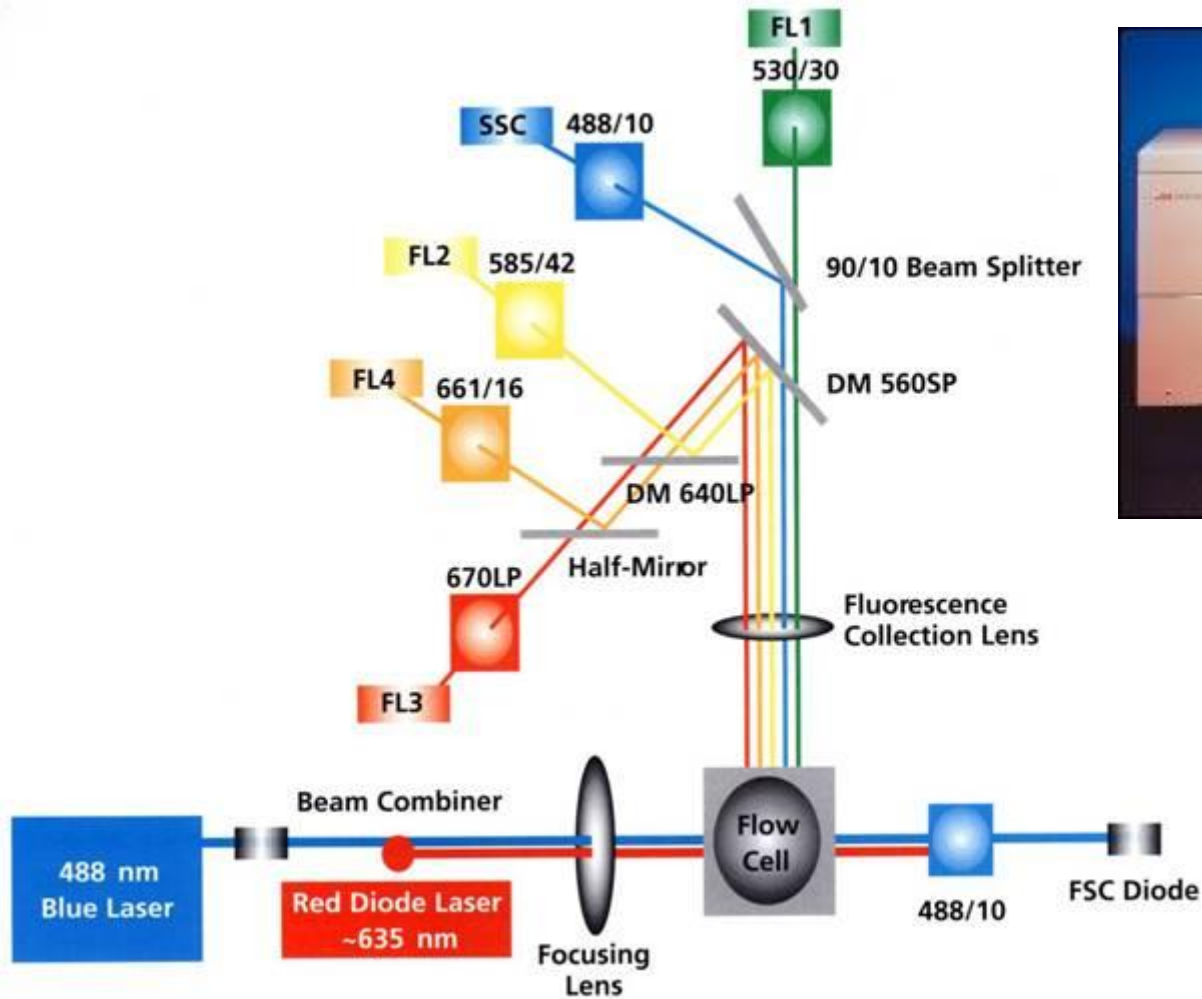
https://en.wikipedia.org/wiki/Avalanche_photodiode



Example Channel Layout for Laser-based Flow Cytometry

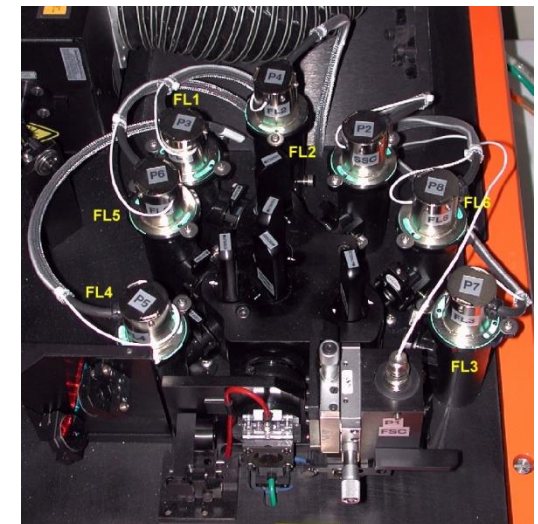
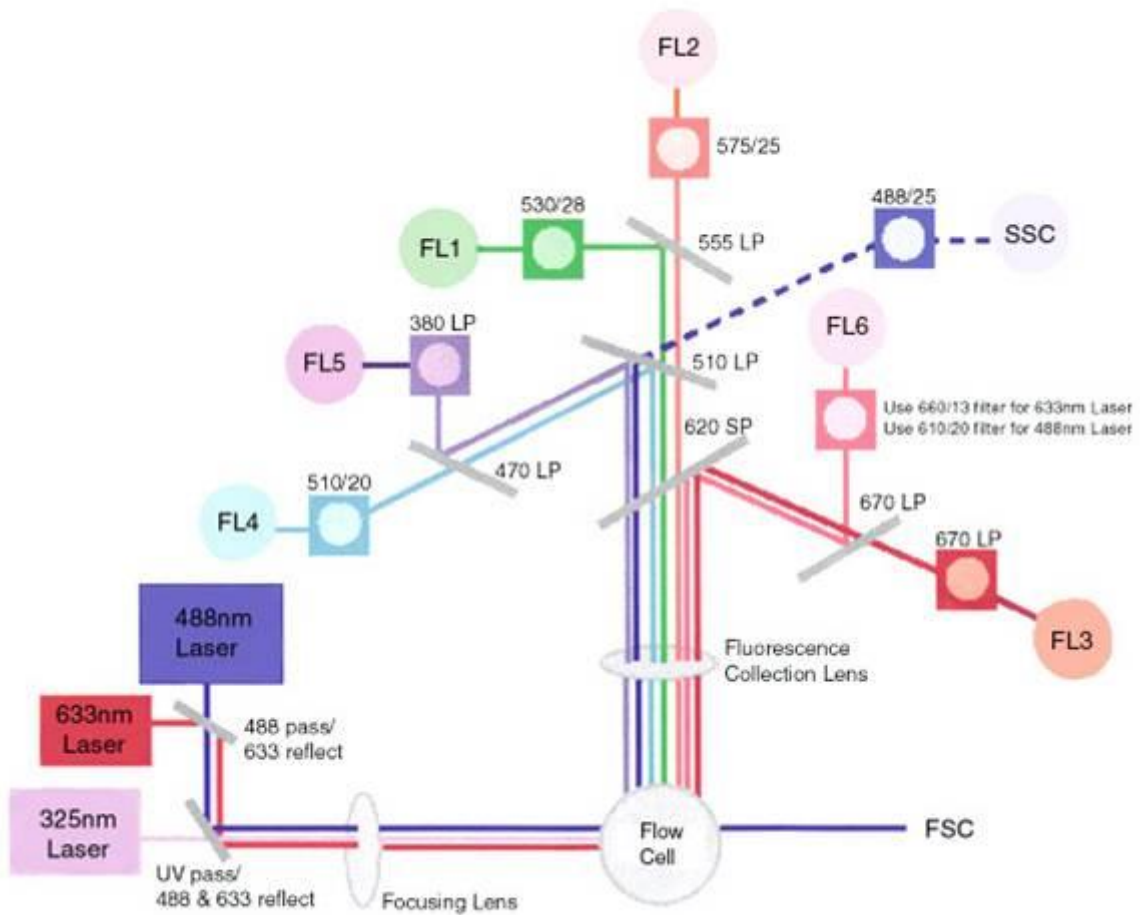


BD FACSCalibur system



http://www.bdbiosciences.com/immunocytometry_systems/

BD LSR II system

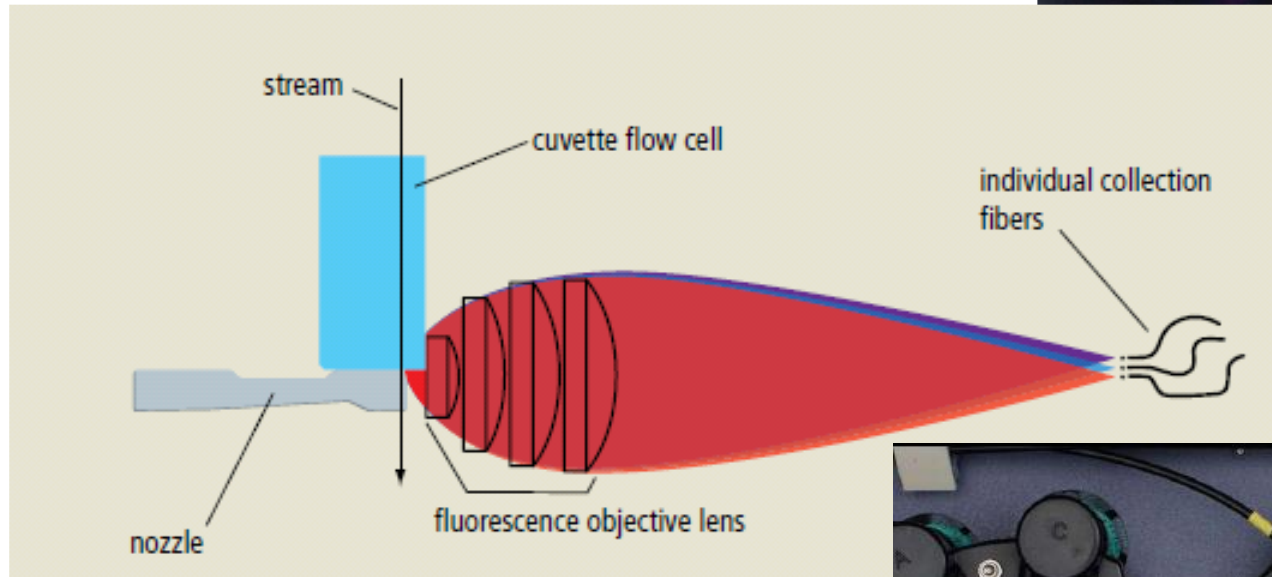


BD FACSVe system



<http://www.bdbiosciences.com/instruments/facsverse/features/index.jsp>

Aria II



SP6800 spectral analyzer

The 405nm, 488nm and 638nm excitation lasers are positioned to reduce fluorescent noise. They enable the system to support 16 or more fluorescent parameters.

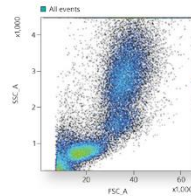
Microfluidics flow cell chip maximizes signal with auto positioning to guarantee high sensitivity. Made of durable plastic with an embedded quartz cuvette, the chip is easy to replace when needed.



The Flowpoint detection system precisely tracks the core stream shape and position in the flow cell as well as the cross sectional position of each passing particle to provide highly reliable measurements. This patented technology visualizes core stability and enables the highest resolution.

Scatter analysis

Forward and Side Scatter parameters to allow relative size and complexity measurements.



Emitted light is directed through a 32 Channel PMT that produces 66 data points of signal detection to analyze emitted photons from 420nm to 800 nm to ensure accurate visualization.



A unique prism collection system

Delivers light through 10 consecutive prisms allowing optimal signal separation while minimizing light loss.

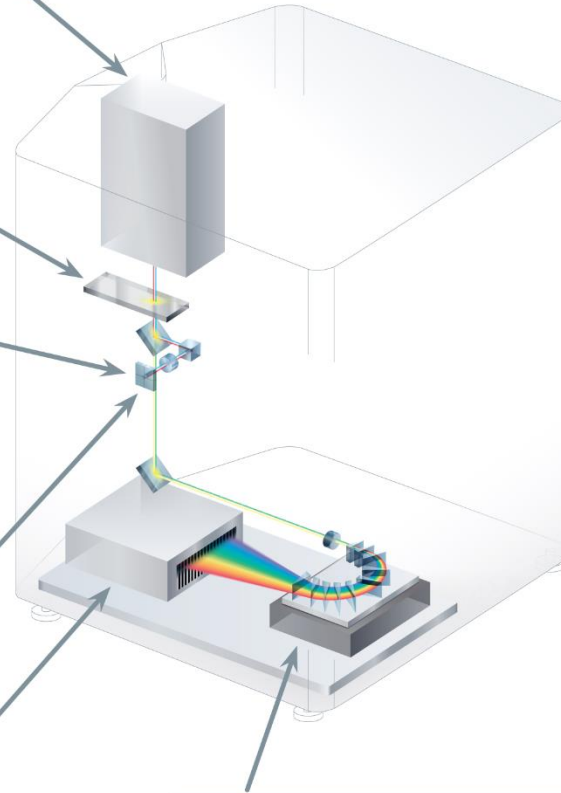
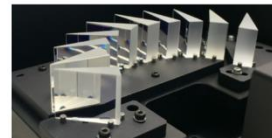
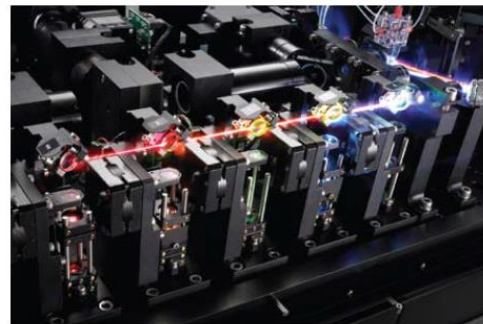


Image Stream & Flowsight Amnis – kombinace průtokové cytometrie a analýzy obrazu

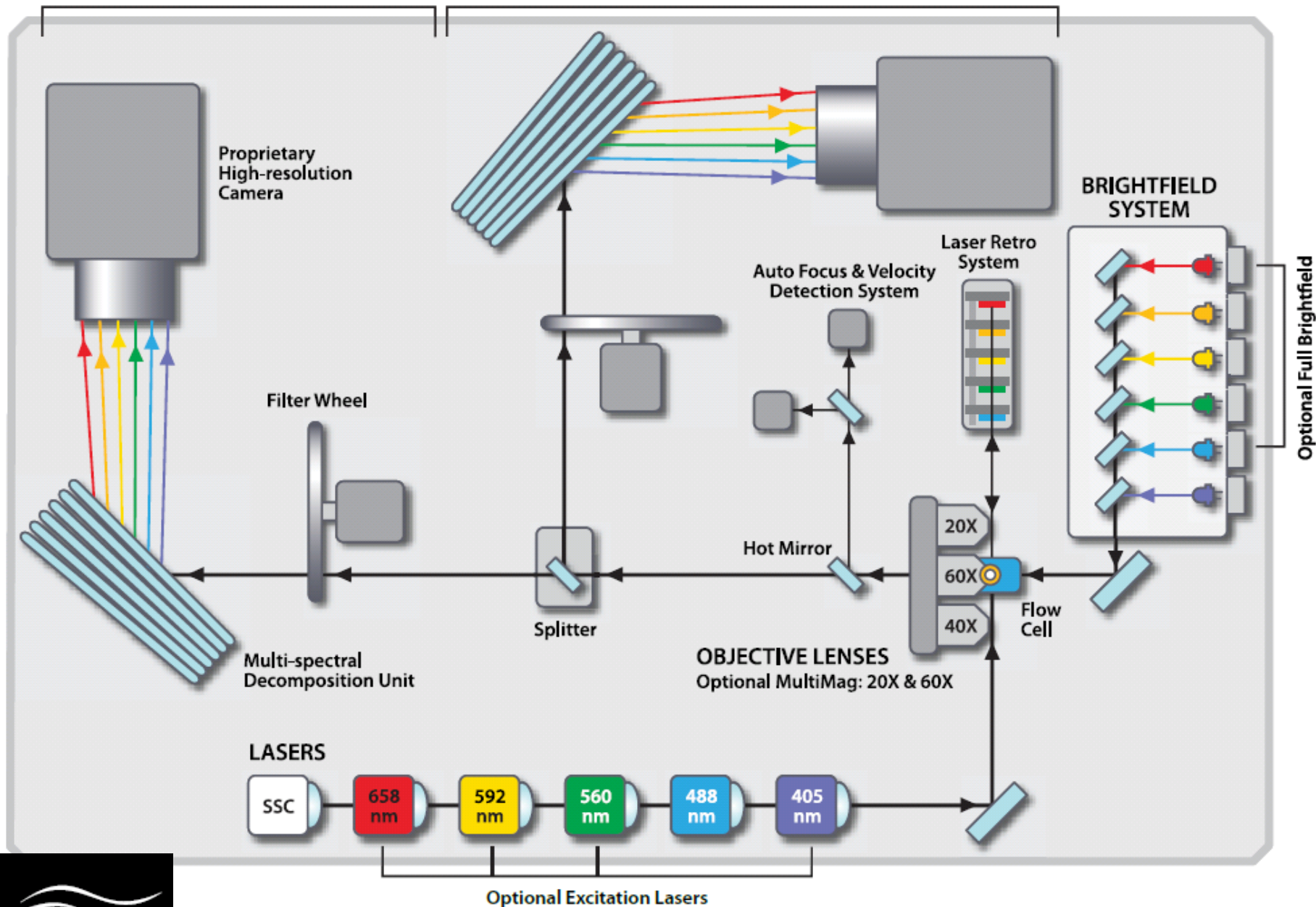


STANDARD COLLECTION SYSTEM

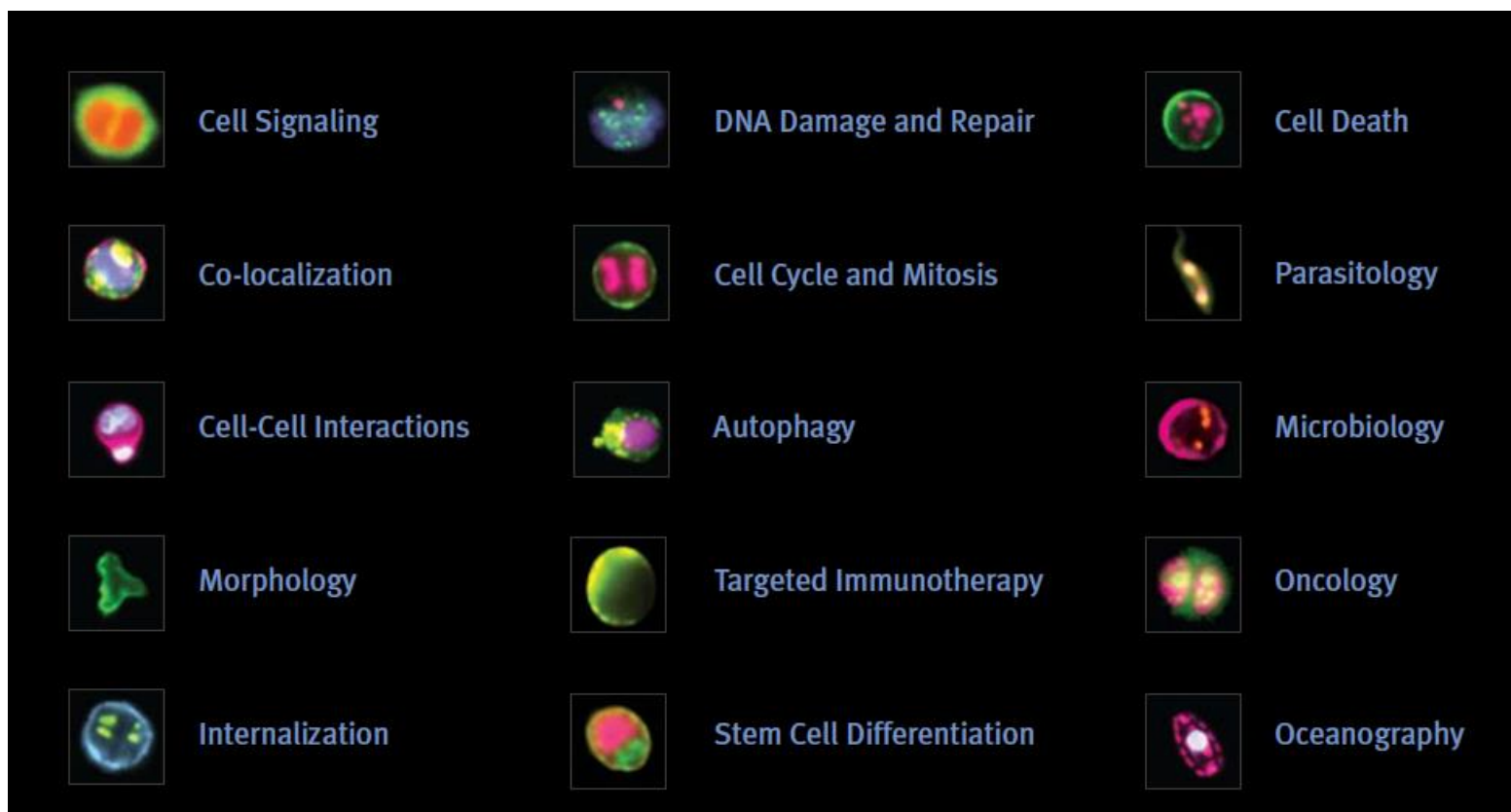
Image Channels: 1-6

OPTIONAL COLLECTION SYSTEM

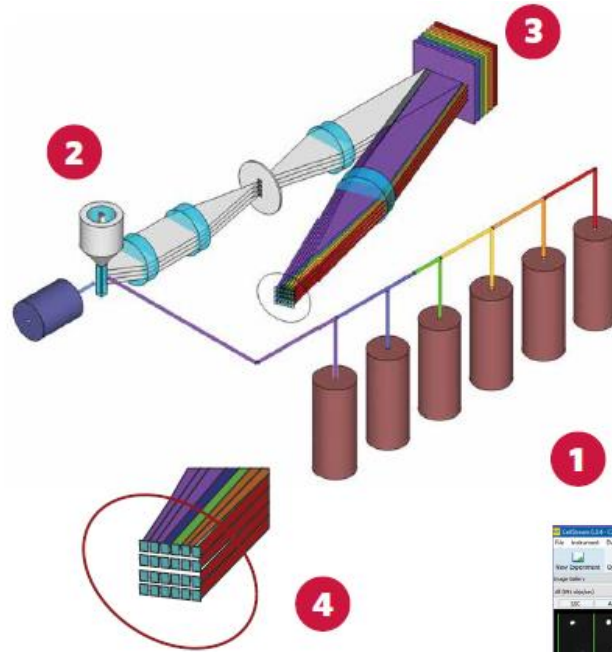
Image Channels: 7-12



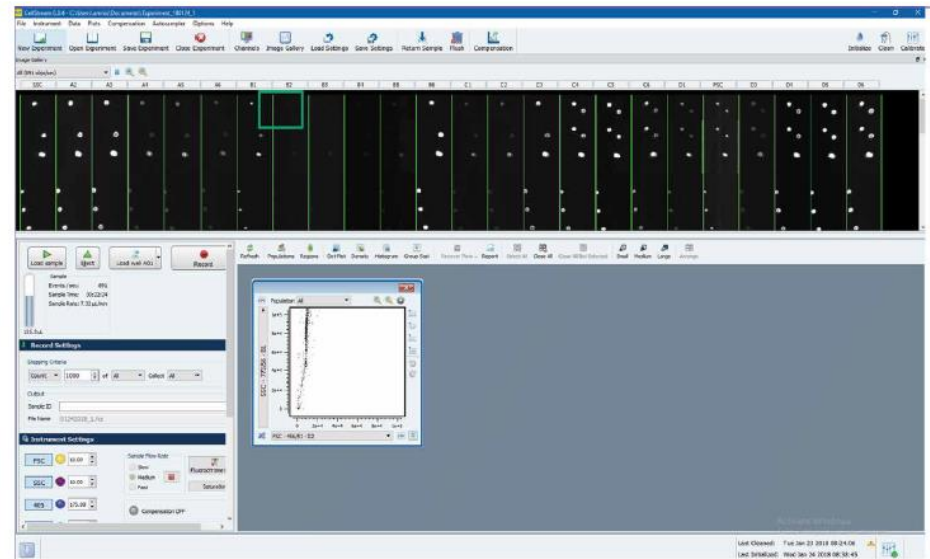
Amnis - aplikace



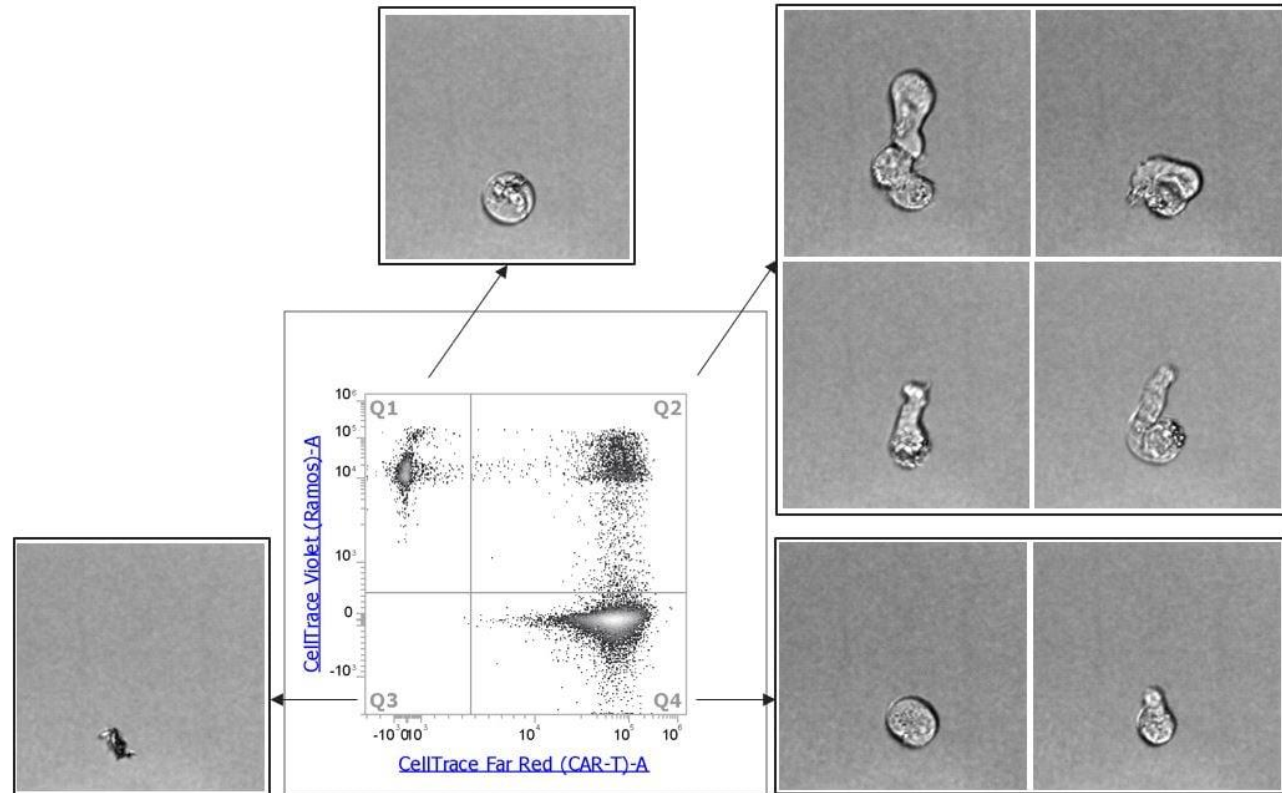
CellStream, Luminex



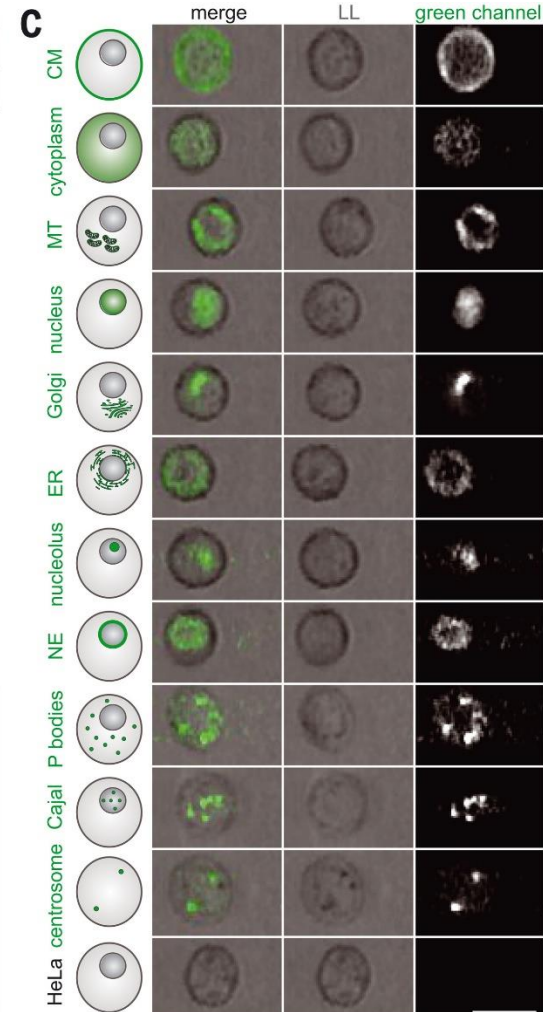
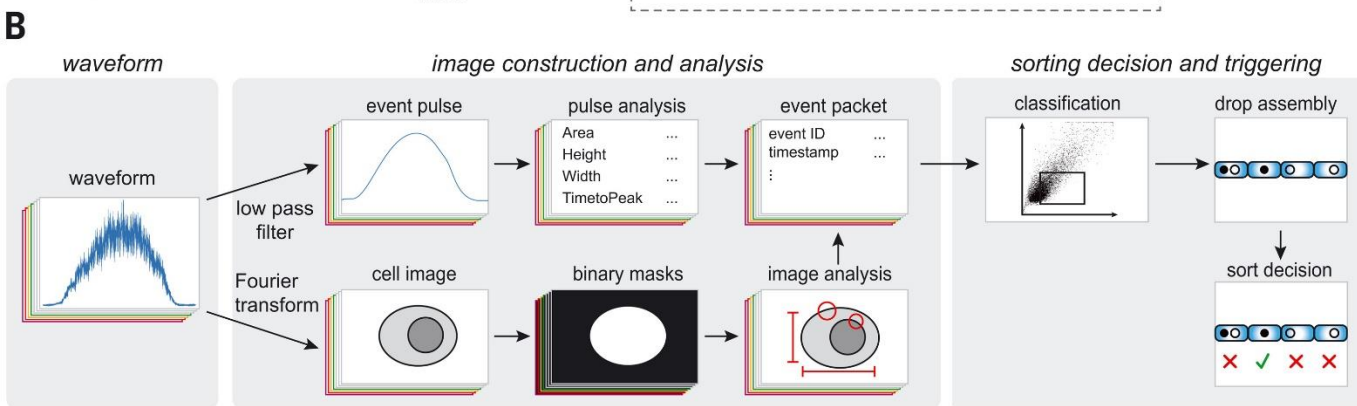
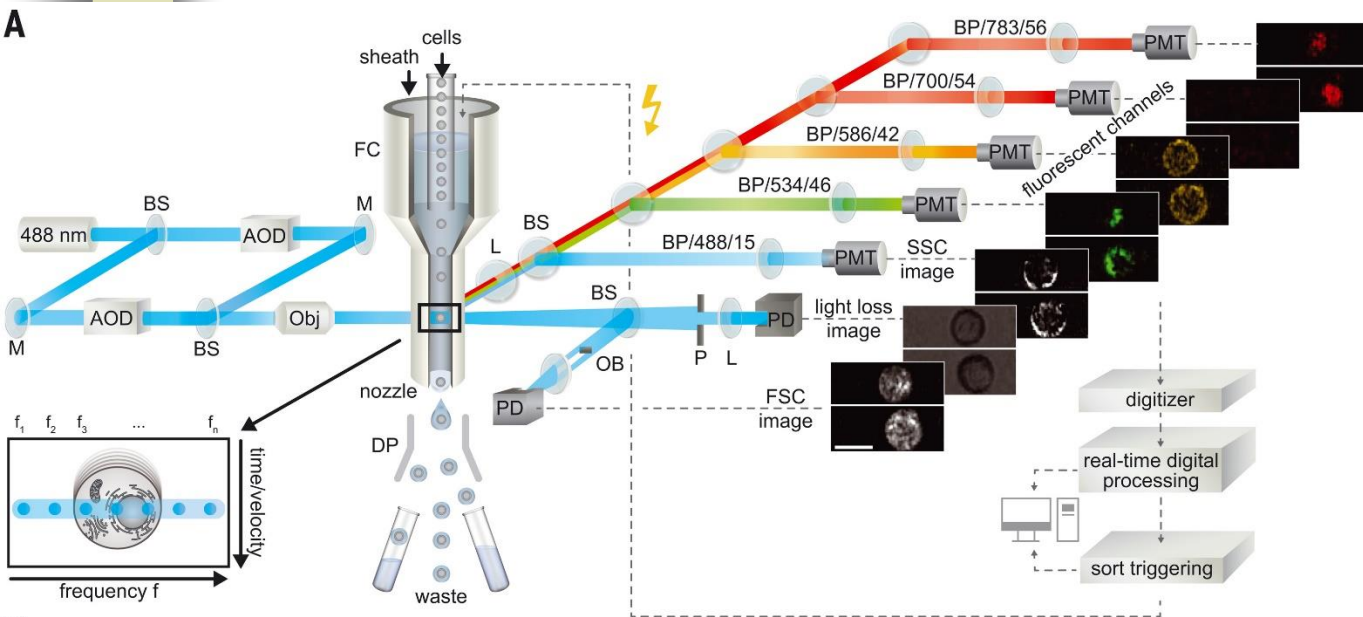
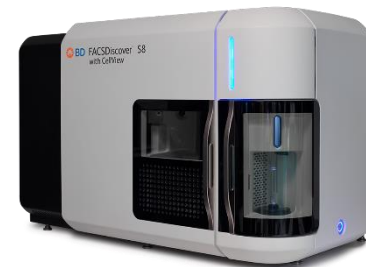
Inside the 7-Laser CellStream® System



ThermoFisherScientific: Attune CytPix Flow Cytometer

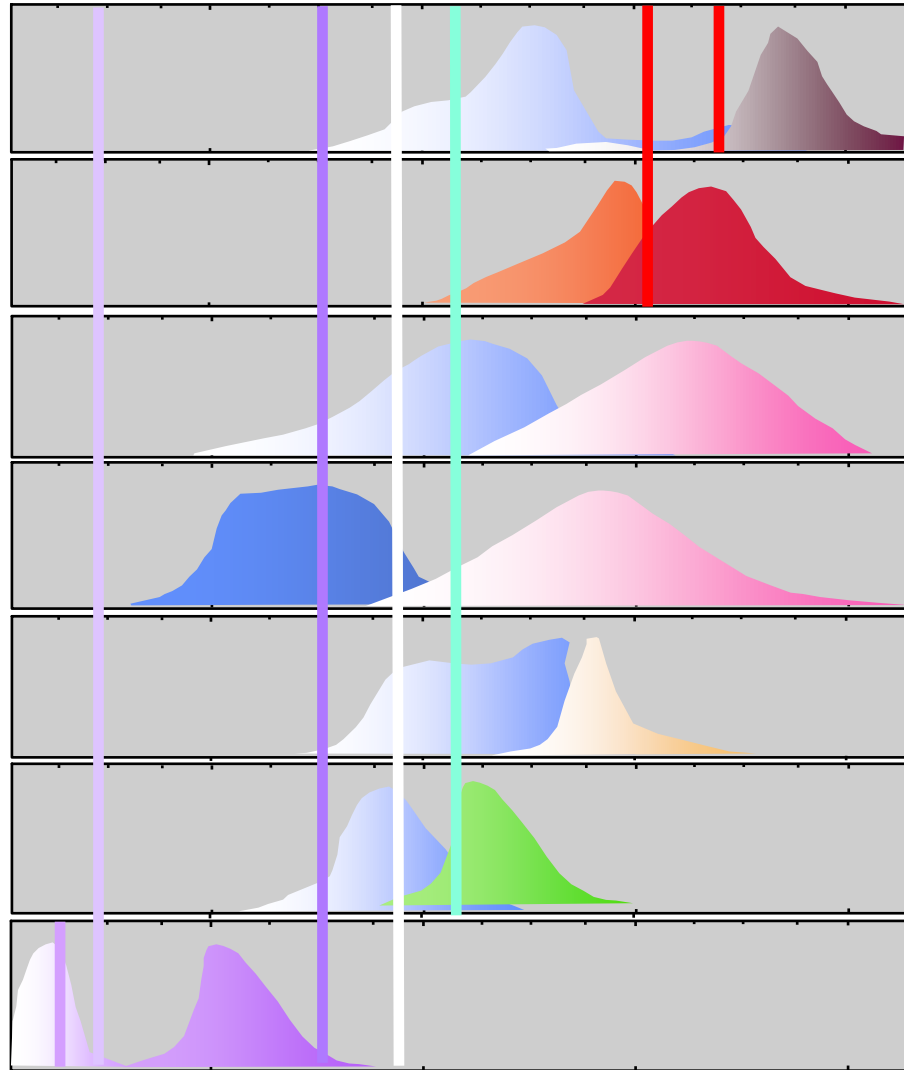


BD FACSDiscover S8



**Common
Laser
Lines**

350 457 488 514 610 632
300 nm 400 nm 500 nm 600 nm 700 nm



PE-TR Conj.

Texas Red

PI

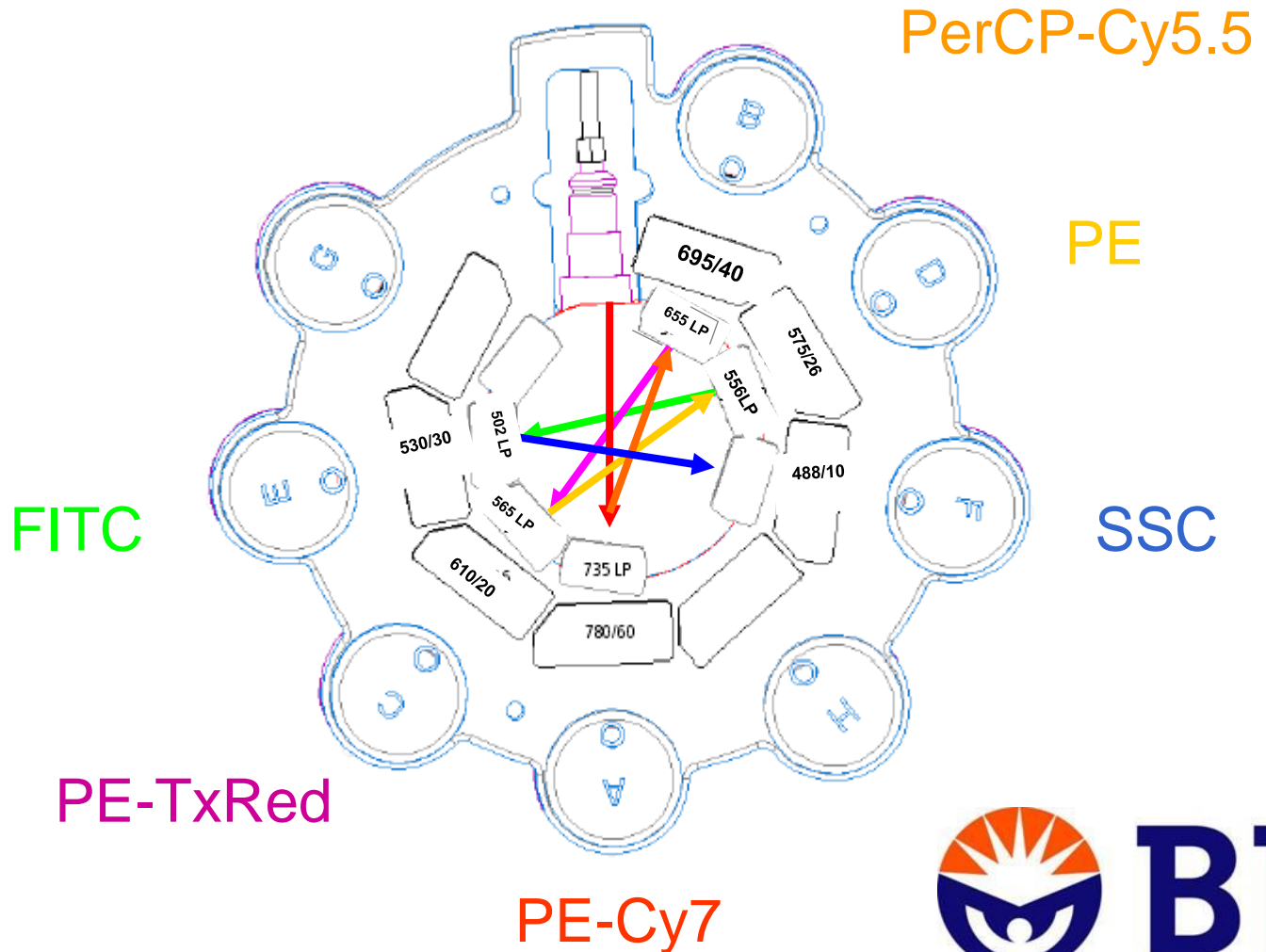
Ethidium

PE

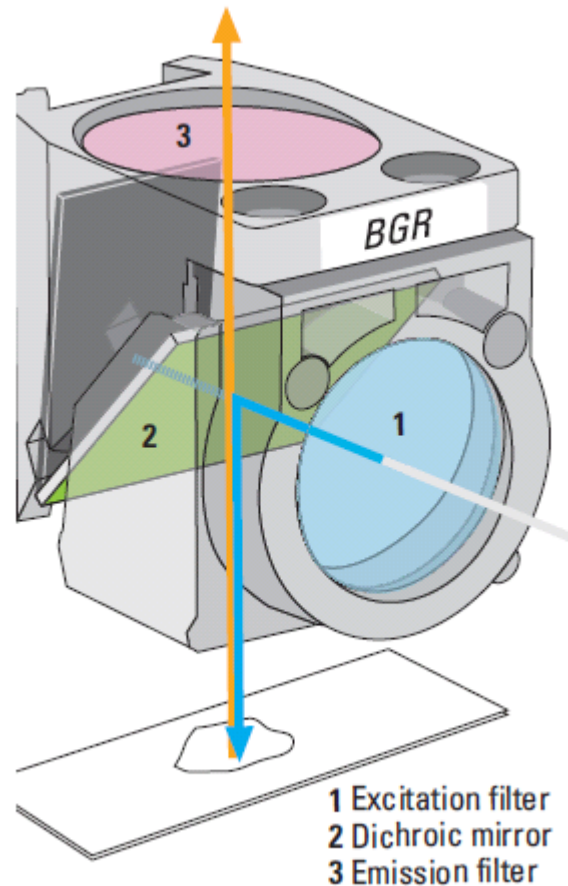
FITC

cis-Parinaric acid

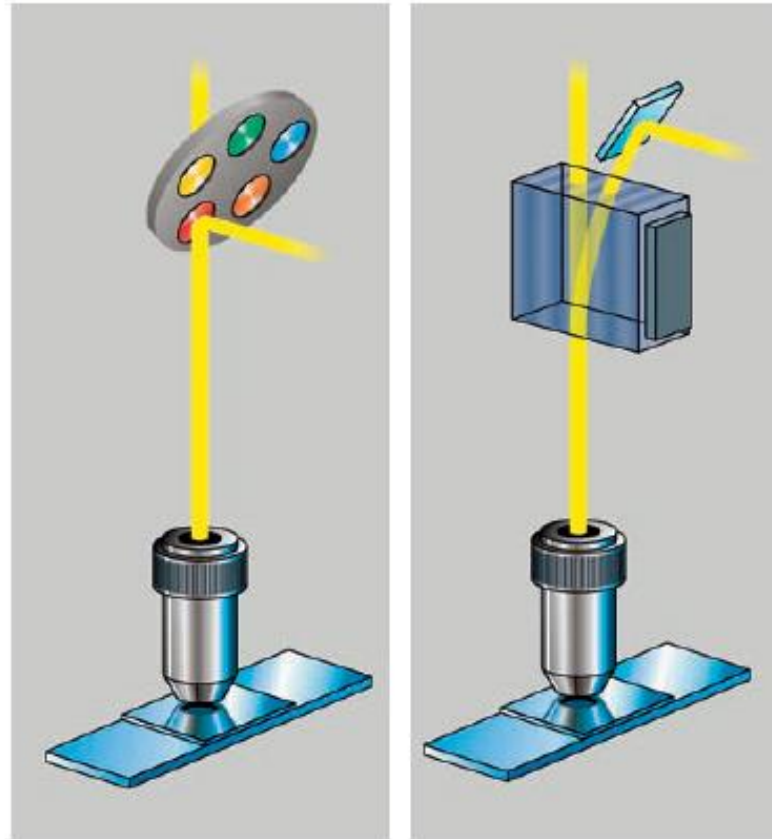
Octagon Detection System



“kostka” pro konvenční fluorescenční mikroskop



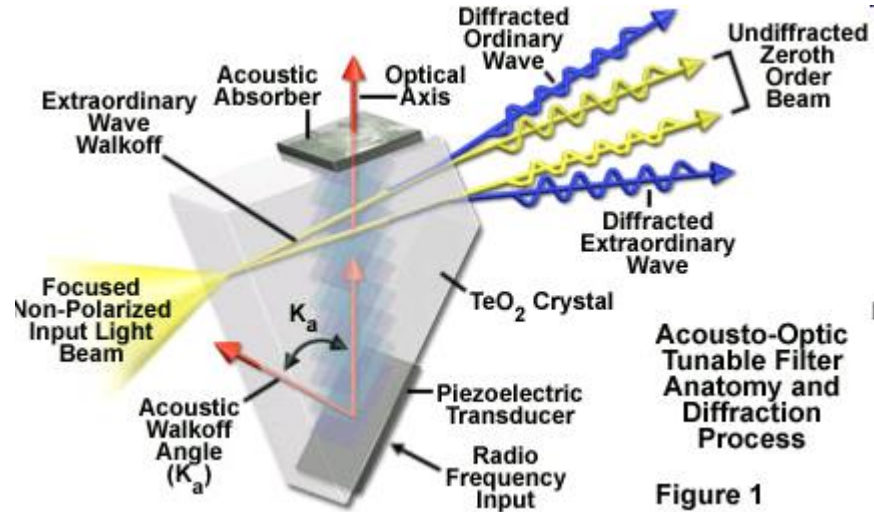
Acousto Optical Beam Splitter AOBS®



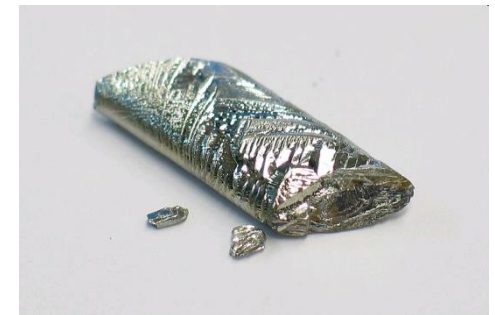
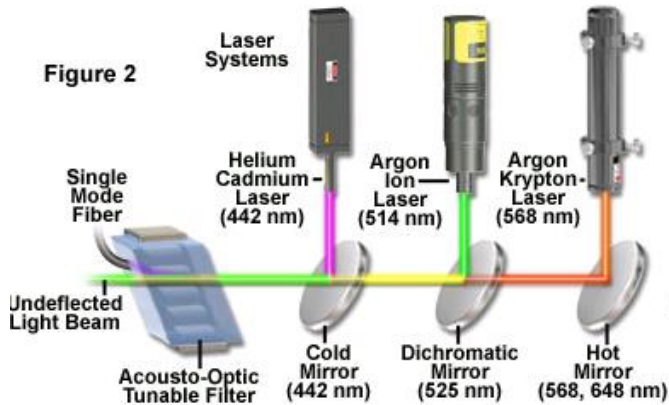
Left: conventional beam splitting by dichroic mirrors requires many optical elements with fixed properties.

Right: the AOBS® is electronically adaptable to all tasks.

Acousto Optical Beam Splitter AOBS®



Acousto-Optic Tunable Filters in Confocal Microscopy

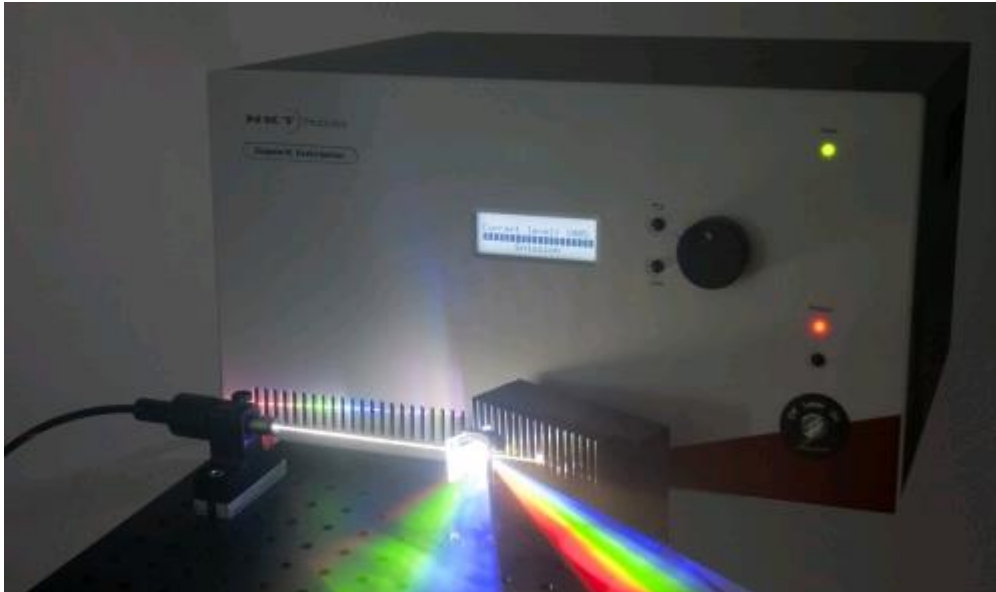


<http://micro.magnet.fsu.edu/primer/java/filters/aotf/index.html>

<http://simple.wikipedia.org/wiki/Tellurium>

Supercontinuum Generation

-a nonlinear process for strong spectral broadening of light



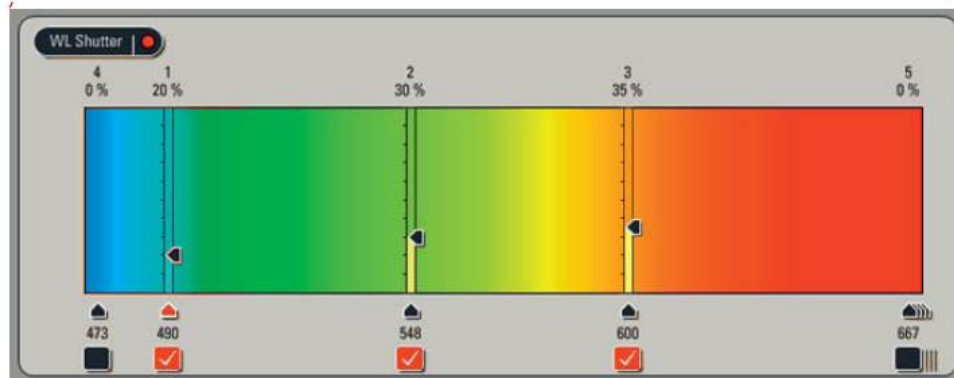
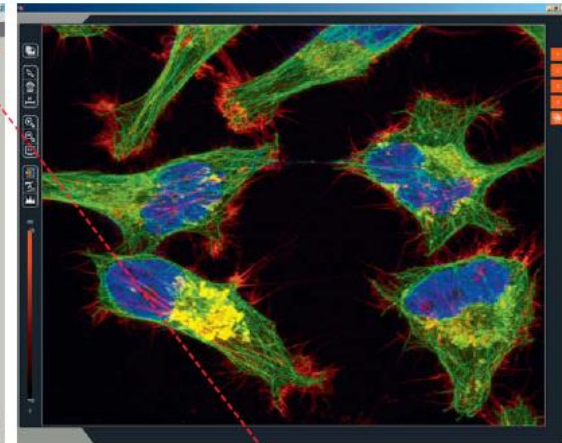
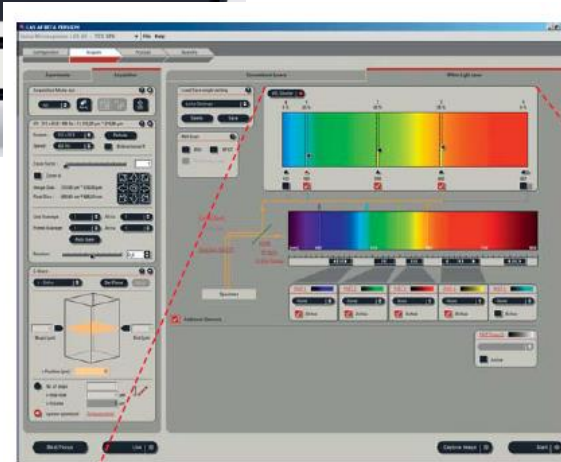
TECHNICAL NOTE

Cytometry
PART A
Journal of the
International Society for
Advancement of Cytometry

Supercontinuum White Light Lasers for Flow Cytometry

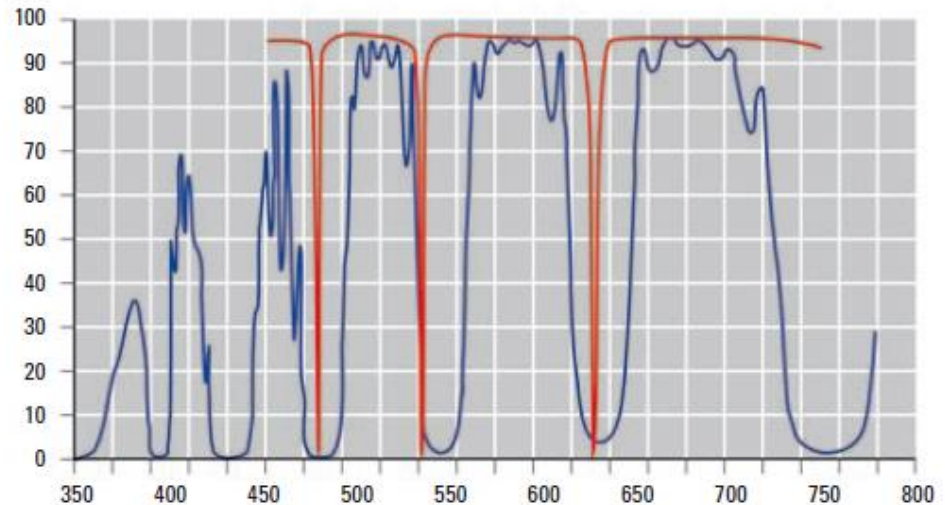
William G. Telford,^{1*} Fedor V. Subach,² Vladislav V. Verkhusha²

Cytometry Part A • 75A: 450–459, 2009



The benefits of AOBS®

- Adaptable to any new dye
- 8 lines simultaneously
- Reflected light imaging
- High transmission
- Truly confocal – real optical sectioning
- Fast switching
- Freely tunable
- Fluorescence correlation spectroscopy with multi-line lasers



Transmission curves

Blue: triple dichroic, blue, green, red

Red: AOBS® tuned to 488, 543, 594, 633 nm

Higher transmission, wider bands and steeper slopes with AOBS®

Fluorescence Spectrum Viewers



<https://www.bdbiosciences.com/en-eu/resources/bd-spectrum-viewer>



<https://www.thermofisher.com/cz/en/home/life-science/cell-analysis/labeling-chemistry/fluorescence-spectraviewer.html>



<http://www.biolegend.com/panelselector>

<http://www.biolegend.com/spectraanalyzer>

<http://www.biolegend.com/webtoolstab>



<https://fluorofinder.com>

